# Nanomaterials in membrane water desalination

Michał Bodzek[a,*], Krystyna Konieczny[b]

[a]*Institute of Environmental Engineering of Polish Academy of Sciences, Marii Curie-Skłodowskiej 34, 41-819 Zabrze, Poland, email: michal.bodzek@ipis.zabrze.pl*
[b]*Silesian Technical University, Poland, email: krystyna.konieczny@polsl.pl*

**A B S T R A C T**

Reverse osmosis (RO) is currently the most important desalination technology and it is experiencing significant growth. This paper reviews the historical and current development of RO membrane materials which are the key determinants of separation performance and water productivity, and hence to define performance targets for those who are developing new RO membrane materials. Given their unique structural and morphological features, nanomaterials have gained considerable attention for their applications in membrane desalination. The emergence of nanotechnology in membrane materials science could offer an attractive alternative to polymeric materials. Hence nanostructured membranes are discussed in this review including zeolite membranes, carbon nanotube, graphene and graphene oxide membranes in their free-standing and composite forms. It is proposed that these novel materials represent the most likely opportunities for enhanced RO desalination performance in the future, but that a number of challenges remain with regard to their practical implementation.

*Keywords:* Reverse osmosis; Nanomaterials; Nanostructured membranes; RO desalination

## 1. Introduction

Most of the water supplies worldwide have traditionally come from groundwater aquifers, rivers and lakes. However, changing climate combined with population growth, economic development, urbanization, large-scale industrialization, and environmental concerns, and limited availability of new and inexpensive freshwater supplies are shifting the water industry's attention to new unconventional water sources. Such scarcity drives us to use lower quality and unconventional water sources, and the treatment and recycling of wastewater (water reuse) as well as desalination of seawater and high-salted groundwater, by far the most abundant global water resource. Desalination has long served as a feasible option to provide safe drinking water in many deserted areas, coastal regions or remote locations [1], offering one of the most important solutions to water deficiency problems.

Beyond mature thermal desalination technologies (multi-stage flash (MSF) and multi-effect distillation (MED), interest has turned to membrane-based technologies because of more favorable energetic (i.e., lower energy consumption). With their outstanding attributes for desalination, membrane desalination technology addresses key issues regarding current and future water shortages. For decades, the desalination plant designs and evaluation of the performances, the conventionally used membrane desalination, particularly for seawater reverse osmosis (SWRO), have been well established to confirm to a complete range of industry standards [2]. However, SWRO is still an energy-intensive technology with associated greenhouse gas emissions and other environmental impacts.

\* Corresponding author.

Nevertheless, despite the overwhelming features of this desalination technologies, the impacts of environments and resource depletion associated with the pretreatment and recovery of the membrane-based desalination still deserve growing attention [3,4]. Although the impact of these issues can be alleviated with good equipment design, operation, practice and maintenance, there are always urgent needs to improve and strengthen the sustainability of this technology [5]. Thus, there is an interest in both the greening of SWRO and emerging technologies beyond SWRO.

Table 1 presents the energy use associated with various water supply alternatives [6].

A lot of improvements in membrane technology and energy recovery equipment over the past 20 y have allowed a two-fold reduction of power needed for seawater desalination [6–8]. The use of desalination for the production of fresh drinking and industrial water significantly increases over the past two decades. The number and size of desalination installations worldwide have been growing at a rate of 5%–6% per year since 2010, which corresponds to an addition of 3.0 to 4.0 million $m^3$/d of new freshwater capacity every year. For example, in the first half of 2008 growth in contracted capacity was 39%, and the total global desalination capacity was about 50 million $m^3$ in 2009 [9] and between June 2015 and July 2016, the new desalination plant production capacity contracted and installed globally was 3.7 million $m^3$/d and the total number of new plants added during this period was 512 [10].

The recent survey stated that a steady increase in demand for a membrane-based desalination market is observed throughout the globe due to its advantage and advancement in the production of low-cost pure water. In addition to this, Global Water Intelligence and International Desalination Association revealed that installed desalination plants around the world have the capacity to produce more than 19.8 billion gallons of freshwater per day [11]. The membrane and the desalination-based industry is a vast portion worth billions. The current desalination market trend is presented in Fig. 1. The freshwater production from membrane-based technology increases significantly over the years. It is also estimated that trend is going to increase drastically in the upcoming days. The noticeable membrane fabricating organizations, such as Toray, CSM, Koch Membrane Systems, Dow-Filmtec, Hydranautics (Nitto Denko) and GE Osmonics, cater to the demand of freshwater crisis [12].

One key for further decreasing the energy consumption of using membranes is to develop novel membrane materials with high permeability. Nevertheless, the current thin-film composite (TFC) reverse osmosis (RO) membranes suffer from a trade-off between salt rejection rate and permeability. To overcome the limits of current polymeric membranes, new types of the membrane with higher permeability and rejection rate have been invented. Membranes with the use of nanoparticles, first of all zeolites, carbon nanotubes (CNTs) and graphene and graphene oxide (GO), can improve the membrane properties and its efficiency [13–15]. Nano-modified membranes could potentially provide a solution to water shortages, as they seem to outperform existing membranes by providing higher water flux and lower energy consumption. Fabrication of membranes with nanoparticles, which have controlled geometry, porosity, and pore shapes, is also challenging [16].

This paper reviews the state-of-art for fabrication and application of desalination membranes with nanoparticles and critically evaluates the advantages and disadvantages of these approaches. Two types of nanomembranes are compared, including free-standing nanomembranes, and mixed (composite) nanomembranes. The prospect of using these novel membranes for water purification is also discussed.

## 2. Current state-of-the-art reverse osmosis technology

RO is today the leading desalination technology and is expected to maintain its leadership in the near future, though new technologies such as membrane distillation [17], electrodialysis [18], capacitive deionization [19] and forward osmosis [20] have been proposed.

Commercial interest in RO technology is increasing globally due to continuous process improvements, which lead to significant cost reductions. These advances include developments in membrane materials and module design, process design, feed pre-treatment, and energy recovery, or reduction in energy consumption. The seven-fold decrease in the salt passage over 30 y has greatly expanded the range of saline feeds that can be treated to meet the stringent potable water standards. The enhanced mechanical, biological and chemical strength of RO membranes, as well as the increased permeability, have reduced the membrane cost per unit volume of water produced by more than 10 times since 1978. The combined effort to salt separation from saline water, minimizing fouling and concentration

Table 1
Energy use of various water supply alternatives

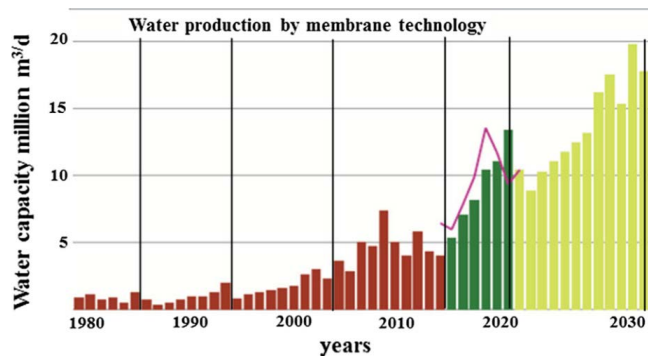| Water supply alternative | Energy use (kWh/$m^3$) |
|---|---|
| Conventional treatment of surface water | 0.2–0.4 |
| Water reclamation | 0.5–1.0 |
| Indirect potable reuse | 1.5–2.0 |
| Brackish water desalination | 1.0–1.5 |
| Desalination of Pacific Ocean water | 2.5–4.0 |



Fig. 1. The market for desalination technology is made by the Global Water Intelligence survey [https://www.desaldata.com/].

polarization, in addition, to maximizing permeate flux and energy recovery requires a significant amount of energy to overcome the naturally occurring osmotic pressure exerted on the RO membranes. SWRO desalination uses several times more energy-intensive than the conventional treatment of freshwater resources [6].

Table 2 provides typical ranges for the cost of freshwater production and energy use of RO membrane systems of medium and large seawater desalination plants with a freshwater production capacity of 40,000 m$^3$/d, or more [6]. As seen from Table 2, SWRO systems of best-in-class seawater desalination plants use between 2.5 and 2.8 kWh of electricity to produce 1 m$^3$ of freshwater, while the industry average energy use is approximately 3.1 kWh/m$^3$. The industry-wide cost for the production of fresh drinking water from seawater at present is approximate 1.1 US$/m$^3$. Energy expenditure typically contributes 25%–40% of this cost depending on the unit power rate and the SWRO plant design, and equipment efficiency.

The systematic long-term testing of full-scale desalination system in the United States (US) shows the lowest energy use that could be achieved with actual highly efficient commercially available desalination equipment and RO membranes at the time of testing (years 2006–2007) was determined to be 1.58 kWh/m$^3$ [21]. That means that the energy consumption decreased from 12 kWh/m$^3$ in the 1970s to less than 2 kWh/m$^3$ in 2006 [9]. Such energy use was measured at RO system recovery of 42% and average SWRO membrane flux of 10.2 L/m$^2$ h. With the integration of energy recovery devices (ERD) in SWRO during the early 1990s, specific energy consumption has been significantly reduced from 5 to 10 kWh/m$^3$ to its present 3–4 kWh/m$^3$ with the most efficient ERD systems [22]. About 85% of this energy is associated with the SWRO process itself, and about 15% are for other SWRO system components (intake, pre- and post-treatment).

Dual media filtration remains the conventional pretreatment process, however, ultrafiltration (UF) pretreatment, UF-SWRO, are becoming more common [23], especially for waters with high impurities. Both UF and dissolved air flotation are receiving increasing attention for their resistance to harmful algal blooms (e.g., at the Gulf of Arabia) [24]. Also, subsurface intakes have recently been applied because of a significant degree of pretreatment. Such a solution acts as a biological filter to remove biodegradable organic carbon and reduce membrane biofouling [25]. Effective pretreatment can affect the energetics of the RO step by reducing fouling.

Given a virtually infinite supply of seawater, SWRO facilities are typically run as one-pass systems with

recoveries of 35%–60% but sometimes is necessary to use a second pass for boron removal [26]. Acid addition and/or antiscalant addition are practiced for scaling control and chlorine–sodium bisulfite for biofouling control, although alternative disinfectants are applied, for example, chloramines (carried through the RO membrane as a residual) or chlorine dioxide (followed by sodium bisulfate before the membrane) as practiced at some RO facility. SWRO trends include larger capacity facilities (e.g., the Sorek facility in Israel, 624 million L/d in 2013), with larger elements (16-in.), vertical orientation for RO membrane modules and pressure vessels (to permit air scouring), and improved operations (fouling control and sensors).

The major environmental impacts of SWRO plants are greenhouse gas (GHG) emissions associated with (fossil fuel) energy use, brine disposal impacts on marine pollution, chemical use, land use, and material use. However, sustainable solutions are available to mitigate these impacts [27]. GHGs can be minimized by renewable energy using. Renewable energy-driven SWRO [28], especially using solar energy (the largest solar-SWRO plant (30,000 m$^3$/d) in the world is under construction in Saudi Arabia), and energy compensation by wind energy in Australia. While the use of renewable energy does not necessarily reduce specific energy consumption, it provides a reduction in GHG emissions. This interest in renewable energy is now evolving toward integrated systems beyond just electricity provided solar photovoltaic panels or wind turbines.

Concentrate discharge can be managed by dispersion through a multiport diffuser system in a suitable marine site, controlling the extent and concentration of the brine [10]. Treatment of all backwashing and cleaning wastes can reduce marine pollution. Chemical use can be minimized by suitable pretreatment (subsurface intakes or UF without coagulant). Furthermore, harmful chemicals can be changed by less toxic, more degradable substances. Material use can be offset by improved recycling and reuse of materials, including SWRO modules.

Nevertheless, the greatest efficiency gains have arisen from the improvement of the membranes. The structure, material, and morphology of RO membranes have been modified to improve functionality (permeability and selectivity) and applicability (mechanical, chemical and biological stability). The current commercial RO membranes are dominated by TFC polyamide (PA) (and its derivatives) membranes consisting of three layers: support (120–150 μm thick), a microporous interlayer (about 40 μm), and an ultra-thin barrier layer on the upper surface (0.2 μm) [29]. Between the barrier layer and the support layer, a micro-porous interlayer of polysulfone is added to

Table 2
Typical cost and energy use for medium and large size SWRO systems [6]

| Water supply alternative | Cost of water (US$/m$^3$) | Energy use (kWh/m$^3$) |
|---|---|---|
| Low-end bracket | 0.5–0.8 | 2.5–2.8 |
| Medium range | 0.9–1.5 | 2.9–3.2 |
| High-end bracket | 1.6–3.0 | 3.3–4.0 |
| Average | 1.1 | 3.1 |

withstand high-pressure compression. The selective barrier layer is most often made of aromatic PA, for example via interfacial polymerization of 1,3-phenylenediamine (also known as 1,3-benzenediamine) and the tri-acid chloride of benzene (trimesoyl chloride) [30]. Membrane pore size is normally less than 0.6 nm to achieve salt rejection consistently higher than 99%. These membranes face critical challenges of relatively low water permeability, low selectivity and high fouling tendency. For example, typical water permeability of commercial TFC RO membranes ranges from ~1–2 L/m² h bar for SWRO membranes and ~2–8 L/m² h bar for brackish water reverse osmosis (BWRO) [31]. Synthesizing novel RO membranes with improved separation properties and better antifouling performance is therefore a key research focus in the field of desalination [32]. With improved chemical resistance and structural robustness, it offers reasonable tolerance to impurities, enhanced durability and easy cleaning characteristics [9,33]. Generally, the development of membrane materials can be divided into two periods according to research activity: (i) the search for a suitable material (chemical composition) and membrane formation mechanism (1960s to late 1980s), and (ii) the evolution of more controlled conditions for membrane formulation to enhance membrane functionality and durability (late 1980s to date) [9].

Several RO membrane manufacturers have developed a new SWRO membrane that includes (i) low fouling membranes, (ii) enhanced boron-rejection membranes, and (iii) inorganic-organic nanocomposite membranes with higher permeability. The main reason was the reduction of specific energy consumption and associated GHG emissions thanks to higher permeability and lower working pressure RO membranes. The fouling-resistant membrane can also significantly reduce energy consumption because transmembrane pressure (TMP) needed to maintain constant RO flux during an operational/cleaning cycle, can have a long time a proper value. Further advances in material science offer the promise of ultra-high permeability RO membranes through a new generation of the nanocomposite, biomimetic (aquaporins), and possibly membranes with zeolite, carbon nanotube or graphene nanoparticle [14,34]. However, there is a limit to lowering energy by increasing permeability because the inherent

osmotic pressure amounted to about 28 bar for seawater, increasing to double at 50% recovery. Operating pressure to overcome RO membrane resistance and provide flux is typically about 10%–20% above the highest osmotic pressure condition in the element/pressure vessel.

While present SWRO practice serves the desalination industry well, it remains an energy-intensive technology with significant environmental impacts.

## 3. Other membrane desalination technologies

There are several emerging low-energy desalination technologies that can potentially achieve a threshold of 2.0 kWh/m³ during seawater desalination [10]. These include forward osmosis (FO) and membrane distillation (MD), and electrochemical desalting processes such as capacitive deionization (CDI) (mostly used for brackish water desalination) [10]. Fig. 2 presents the differences between these processes [10].

FO is an osmotic-pressure gradient driven process, which involves the extraction of water from a lower-osmotic pressure feed solution into a higher-osmotic pressure draw solution across an FO membrane. FO has drawbacks in relation to fabricating high-performance membranes that also ensure minimal internal concentration polarization [35,36]. Internal concentration polarization in FO is caused by salt diffusion into the porous space of the membrane's support layer and causes a severe reduction in flux [36]. For FO, there has been significant progress in the evolution of higher-flux, lower-salt leakage, commercially-available FO membranes, with an aquaporin FO membrane. We observed also recent progress in developing hollow-fiber FO membranes [37,38]; with the flux of >40 L/m²h against a draw solution of 2 M NaCl [38]. Progress is also evident in devising more effective draw solutions, driven by the goals of higher osmotic pressure, lower reverse draw solute flux, easy regeneration, non-toxic, and lower cost. The carbon dioxide-ammonia thermolytic draw solution has evolved into commercial applications [39], with temperature-sensitive hydrogels showing promise as a draw solution. Moreover, low-grade waste heat (e.g., 60°C) is adequate to recirculate these thermolytic components [40]. Several commercial FO companies are (i) operating in niche
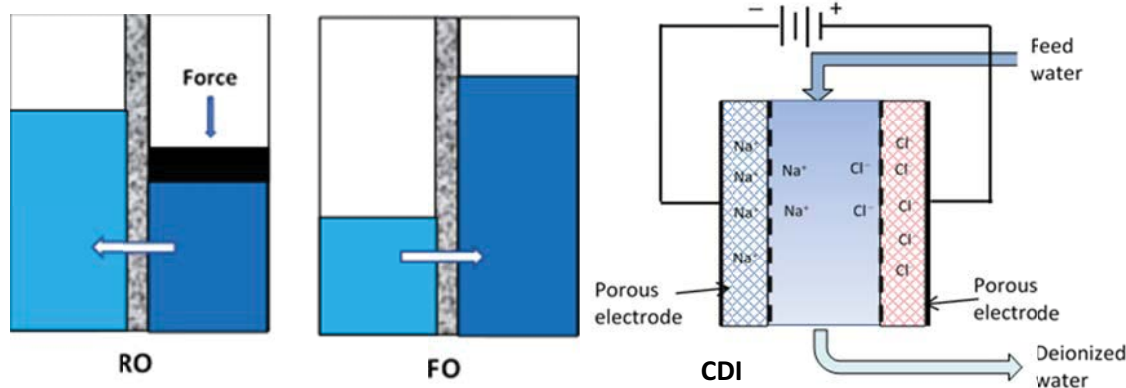


Fig. 2. Schemes of various membrane processes.

applications (e.g., brine concentration), (ii) fabricating FO membranes (presently limited to flat sheet/spiral wound/plate-and frame membranes/modules), and (iii) marketing thermolytic draw solutions (utilizing waste heat for component recirculation). The FO process itself can directly desalt seawater as a feed solution by employing a higher-osmotic pressure draw solution, however, the energy consumption of product water recovery and draw solution recirculation are not low [41]. The energetic of the FO process can increase if coupled with low-pressure reverse osmosis (LPRO) [20,42], in which indirect desalination is achieved. The FO step dilutes seawater (acting as a draw solution) with water of low quality (e.g., effluent after secondary wastewater treatment) acting as a feed solution, and the diluted draw solution than further processed by LPRO (Fig. 3). The FO-RO sequence provides a double barrier for organic micropollutants and pathogens in the wastewater which, as a result, is a water recovery from wastewater (water reuse) [43]. The resultant concentrated feed solution can potentially be treated by an anaerobic process with a biogas production of about 1.5 kWh/m³ for FO concentration factor of 1 [43], and further can decrease the energy consumption of the overall FO-LPRO system. Valladares Linares et al. [44] showed that compared to SWRO, the FO-LPRO system has a higher capital cost but a significantly lower operations cost due to savings in energy consumption and fouling control, with a lower unit cost of produces water.

Summing up, Shaefer et al. [45] have stated that the "FO process is not intended to replace RO, but rather is to be used to process feed waters that cannot be treated by RO", so the hybrid system FO-LPRO is the step which provides pretreatment (salinity and fouling reduction) for the subsequent LPRO step.

MD is a membrane process, driven by a thermal (temperature) gradient, with water vapor transported across a hydrophobic microporous membrane using a significantly lower temperature than conventional distillation at very low operating pressures (nearly 1 bar). Advantages of the MD process are that product-water distillate flux and quality (<10 ppm) are insensitive to feed-water salinity up to about 200,000 ppm [46,47], it is less prone to fouling than



Fig. 3. FO-RO/NF/MD system for water desalination.

pressure-driven membranes [47], and it requires a small footprint. Depending on operational conditions, water recovery can reach (more than) 90%. Current MD membranes synthesized from polytetrafluoroethylene (PTFE) and polyvinylidene fluoride (PVDF) face challenges in cost, sufficient porosity and low flux compared to membranes applied in RO; therefore, fabrication of high-performance novel MD membranes that can compete with RO may help increase the future application of MD in desalination. In a further improvement of the process are MD membranes with higher flux, higher hydrophobicity (contact angle), and lower wettability and appropriate process configuration [48,49]. Recent progress has been made in fabricating hollow fiber and multi-bore MD membranes [50]. Module scale-up with efficient internal heat recovery and satisfactory flux remains one of the main challenges of the MD process [51,52]. Some companies propose water-treatment hollow fiber microfiltration (MF) membranes as MD membranes, but they do not always possess the desired properties. That is why MD units with different configurations and capacities use flat-sheet membranes [10].

MD requires thermal energy to drive the separation process and electrical to move feed, product, and brine flows. MD can meet the energy threshold if powered by waste heat to satisfy the thermal power requirement (>100 kWh/m³) [49], with only about 1.0 kWh/m³ of electrical power. It is a necessity to integrate waste heat recovery and utilization into the overall MD system. When coupled with solar energy or geothermal energy, a hybrid MD system can provide a reduction in GHG emissions. Fouling in MD is significantly lower than in conventional pressure-driven membrane separation, and scale inhibitor and acid may be required to prevent scaling.

CDI is a technology to deionize water by applying an electrical potential difference over two electrodes, which are often made of porous carbon. Anions, ions with a negative charge, are removed from the water and are stored in the positively polarized electrode. Likewise, cations (positive charge) are stored in the cathode, which is the negatively polarized electrode [53]. The CDI apparatus used consisted of two electrodes that formed a capacitor, across which a voltage was applied to adsorb ions of opposite polarity from a stream of salty water (Fig. 2). When the applied potential was reversed, the salt was then released in the form of a concentrated brine solution. The physical properties of CDI electrodes involved in ion adsorption significantly affect the dynamics of the CDI process [53]. The CDI electrode material must have a large surface area to allow the accumulation of ions and high electrical conductivity, high capacity and reasonable porosity to guarantee the adsorption of ions in the electrode structure [53,54]. Carbon-based materials have been shown to have such properties and have been documented as potential electrode materials in CDI applications in the form of carbon aerogels [55], carbon sheets [56] or carbon nanotubes [54,57,58]. Compared to RO and distillation, CDI is considered to be an energy-efficient technology for brackish water desalination. This is mainly because CDI removes the salt ions from the water, while the other technologies extract the water from the salt solution.

All of the discussed membrane processes, conventional and emerging, have inherent fouling challenges and
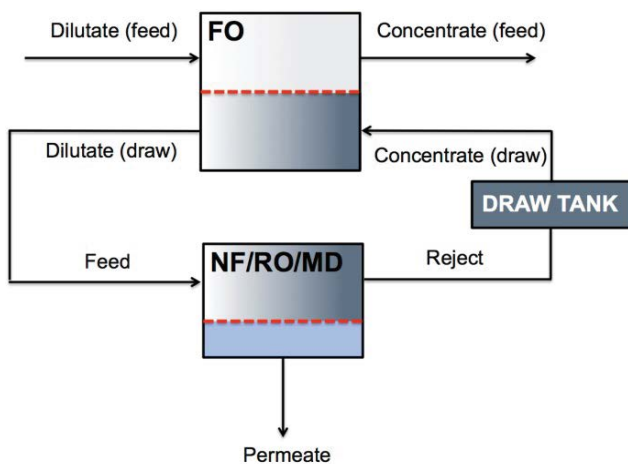
associated pretreatment requirements. However, these vary among processes, for example, FO is less prone to irreversible fouling than RO and requires less pretreatment [20] whereas scaling represents the main challenge for MD vs. biofouling for RO. Discussion is ongoing whether any of the aforementioned processes will, in the near or even the long term, replace SWRO as the conventional seawater desalination technology. However, there are other niche applications, for example, (i) use of FO in brine concentration in managing produced water from fracking and (ii) use of MD in brine concentration and a step toward zero liquid discharge (ZLD) in inland desalting applications [6]. Among the many possible hybrid systems, potential hybrids of interest include: (i) the FO-LPRO hybrids for indirect seawater desalination; (ii) FO-MD in which (waste heat-driven) MD plays a role in recycling draw solution components; and (iii) MSF (or MED) MD in which the latent heat of the thermal brine is used to recover additional water [10].

## 4. Nanomaterials in water desalination

As mentioned above, the application of the conventionally used RO membranes has been severely restricted by the unsatisfactory water recovery and high-pressure operation, especially while generating substantial amounts of liquid wastes. Therefore, the development of the next-generation of low-pressure membranes with low energy consumption and heightened salt rejection is needed to provide a viable route for sustainable membrane desalination [2]. Exciting findings and breakthroughs have been constantly made through the incorporation of nano-inorganic nanomaterials as zeolites, metal oxides, silica, nano-clay and metal–organic framework to the manufacture of nanocomposite membrane to enhance the membrane physicochemical properties and execution [14,59–63]. Among them, zeolite, carbon nanotube- and graphene-based nanomaterials are reflected as the huge potential and prominent contenders for the advancement of the membrane separation process [64–68].

### 4.1. Zeolite membranes

Zeolites are crystalline aluminosilicate materials with uniform subnanometer- or nanometer-scale pores, that is, 0.3–0.8 nm [69]. Zeolites have a three-dimensional framework structure that forms uniformly sized pores of molecular dimensions. Those pores act as sieves on a molecular scale, which means they selectively allow molecules that fit inside the pores to pass while excluding molecules that are too large. Zeolites are produced industrially in large quantities but are also available naturally.

Three forms of zeolite membranes have been prepared and studied, that is, an individual zeolite layer, zeolite crystals in the polymer membrane matrix, and a monolithic zeolite layer on support [70]. Zeolite membranes pose unique properties for wide applications such as membrane reactors [71], gas separation [72], fuel cells [73], pervaporation (PV) [74], and desalination [75,76]. The most used methods to synthesize zeolites that can be used to obtain zeolite membranes are in-situ crystallization, secondary growth, and vapor phase conversion [70,77]. In the first method, hydrated silica and alumina in form of gel are cast on a support to form the zeolite crystalline structure under certain temperature conditions [70]. In the secondary growth method, the process consists of two stages: nucleation and growth of the crystals. The last method, the vapor phase conversion, consists of the crystallization of amorphous aluminosilicates into zeolites through their contact with vapors of organic substances and water in autoclaves [70]. Fig. 4 shows the sub-nm inter-crystalline pores within the zeolite structure that allow the passage of water molecules and rejects the salt [69], and Fig. 5 zeolite nanocomposite membrane [78].

### 4.1.1. Zeolite membranes in RO desalination

Zeolite membranes have high thermal and mechanical properties, which make them suitable for different desalination processes. For instance, RO membranes should withstand high pressure and MD membranes should tolerate high temperature. Increasing the TMP can enhance both the water flux and ion rejection because the ion flux is much less affected by pressure compared to the water flux. When high pressure and temperature affect RO and MD membrane properties, operating at elevated temperatures and high hydraulic pressures is desirable for enhancing the separation efficiency using zeolite membranes [78]. Because of their high cost, zeolite membranes in desalination are currently used where polymeric membranes cannot be used. However, many experimental studies have been done to evaluate the potential of zeolite membranes. Molecular dynamic simulation studies showed that zeolite membranes could theoretically remove ions from aqueous solutions by RO processes. Theoretical calculations have shown that ions can be completely excluded by zeolite membranes with pore sizes smaller than the size of the hydrated ion. A-type zeolite membranes have 0.4 nm pores and MFI (mobil five) type membranes 0.56 nm. The first experimental attempt at RO of a NaCl solution using a MFI silicalite-1 zeolite membrane showed 77% salt rejection and a water flux as low as 0.003 m³/m² d at 21 bar. It is also reported that the rejection of divalent cations was higher than for monovalent ions. In other words, the rejection of sodium ions in a mixed ion
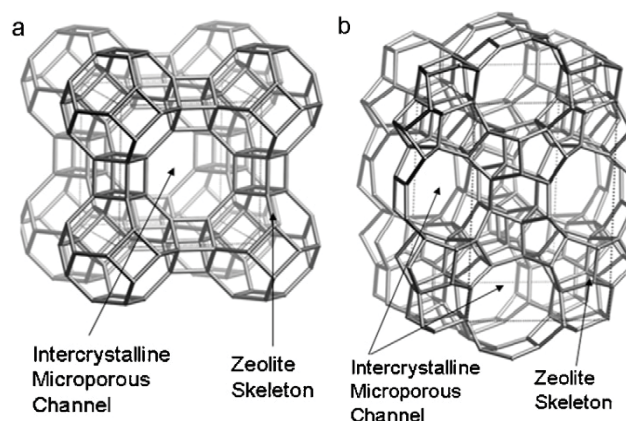


Fig. 4. Micro-porous ceramic membrane structure: micro-porous channel in the crystalline structure: (a) Type A zeolite and (b) MFI zeolite) [69,78].
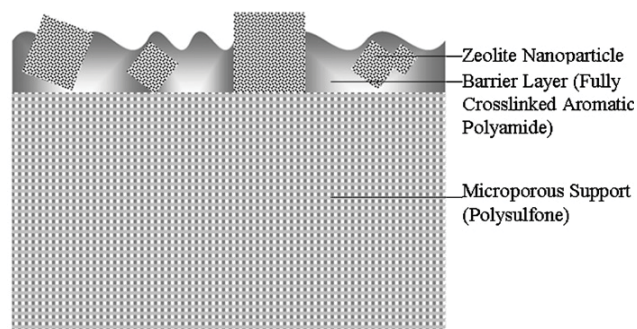
Fig. 5. Schematic cross-section of zeolite nanocomposite membrane [78].

solution was lower than that for a pure solution of NaCl. These results show that the filtration mechanism is not only dependent on size exclusion, but also on Donnan exclusion due to the charged double layer induced by adsorbed ions on the pore or the inter-crystalline walls [79].

Although the first RO test with a zeolite membrane was unsuccessful, that is, both salt rejection and water flux were too low for practical use. Modifying the zeolite structure, first of all, the optimizing Si/Al ratio, which dominates the wettability and membrane surface charge, flux and salt rejection can be improved. The Al content in the membrane influences the surface hydrophilicity and therefore affinity with water [80]. Defects in the crystal structure are minimized by the secondary growth of a zeolite layer on zeolite seeded onto a porous $\alpha$-alumina substrate [81]. This combined effort generated a remarkable improvement, with a 2 μm thick zeolite membrane with a 50:50 Si/Al ratio rejecting 92.9% of sodium ions with a water flux of 1.129 kg/m²h at 28 bar [82]. In a recent report, the thickness of the membrane has been further reduced to 0.7 μm, providing excellent organic (>99%) and salt rejection (97.3%) as well as nearly 4 times improvement in water flux [83].

RO membranes synthesized with hydroxysodalite (HS) zeolite simultaneous removed ions and dissolved organics from water [84]. Results at an optimum feed flow rate of 3 L/min, feed temperature of 60°C, and TMP of 3 bar, permeate flux the tested HS zeolite membrane amounted to 4 L/m²h.

Fathizadeh et al. [85] studied the effect of NaX nano-zeolite addition into polyamide as a top thin layer of membrane on water flux and salt rejection in a RO process. Compared to the polyamide membranes without NaX, the prepared membranes had higher water permeability and were more thermally stable, due to the increase of pore size, improving the surface properties indicated by roughness, contact angle, and solid–liquid interfacial free energy. However, the obtained salt rejection was low. Experimental results showed that the nanocomposite zeolite membrane containing 0.2% (w/v) nano-NaX zeolite had a water flux higher by 1.8 times than the water flux of the pure polyamide membrane [85].

Liu et al. [86] using MFI-type zeolite membranes for separation of organics/water mixture showed how ionic species and dynamic size of dissolved organics highly affect the organic rejection performance. For electrolytes, the zeolite membrane achieved separation efficiency of 96.5%

with a water flux of 0.33 L/m²h, and for non-electrolytes separation efficiency was 99.5% and 17% for 100 ppm of toluene and 100 ppm of ethanol, respectively indicating higher separation efficiency for the organics with higher molecular dynamic size [86]. Also, Rassoulinejad-Mousavi et al. [87] studied zeolite MFI as a nanostructured membrane to remove hazardous chemicals from a contaminated water solution. A non-equilibrium molecular dynamics analysis was performed to see the potentials of the zeolite porous nanosheet to separate the mercury chloride ($HgCl_2$) and copper chloride ($CuCl_2$) from water as two major hazardous contaminants. A RO system was simulated and tested at different induced pressures from 10 to 200 MPa. Ion removal, water flux, water molecules accumulation at different locations, number of hydrogen bonds, Van der Waals interactions, ions tracking path and radial distribution function between water molecules and the ions, were investigated in detail. The results indicated that the zeolite MFI nano-membrane can effectively prevent mercury, copper and chlorine ions from permeation while keeping a large water flux through the membrane. This behavior of the zeolite introduces a competitive candidate for the water purification industry and sets it apart from other nanostructured membranes.

Some recent results of zeolite membranes applications in desalination are provided in Table 3.

### 4.1.2. Challenges and opportunities of application of zeolite in desalination

In the last decade, the significant advances that have been made for zeolite membrane synthesis, preparations, characterization, and modifications have increased their opportunities and applications in different areas, desalination included. Synthesis of high water flux, defect-free, thin zeolite membranes was possible thanks to the understanding of separation mechanisms during transport through zeolite membranes. Crystallization of oriented zeolite layers on supports and the appropriate use of microwave heating, as well as the development of thin supported zeolite layers, seems to be the most promising tool in zeolite membrane preparation [92]. An additional opportunity for the zeolite membrane is the growth of oriented microcrystals in the zeolite layer, which results in enhancing mass transport and controlling the thermal stress [93]. Nevertheless, zeolite membranes and the use of zeolite materials for membrane preparation still face some challenges.

The scaling up of zeolite membranes should also be solved. Moreover, long-term stability, membrane reliability, and cost reduction of zeolite membranes should be further improved to allow for higher applicability on an industrial scale. Permeability data of zeolite membranes are also conflicting. While many studies have shown high water permeability of zeolite membranes [94], many others reported very low water flux [95]. On one side, when compared with commercial PA membranes, both molecular dynamics simulations and experimental results showed much lower permeability of zeolite 4A membranes [96]. The commercial PA membranes have 10-folds higher permeability than that of zeolite 4A membranes [96]. On the other hand, the new concepts to integrate the zeolite nanoparticles

Table 3
Recent applications of zeolite membranes in desalination

| Materials | Operating conditions | Performance results | References |
|---|---|---|---|
| MFI-type zeolites | 0.1 M NaCl feed water; 2.07 MPa; 0.1 M NaCl + 0.1 M KCl + 0.1 M NH$_4$Cl + 0.1 M CaCl$_2$ + 0.1 M MgCl$_2$ at 2.4 MPa | Flux 0.112 L/m$^2$ h; Na$^+$ rejection 76%; flux 0.0.058 L/m$^2$ h; rejection: 58.1% Na$^+$; 62.6% K$^+$; 79.9% NH$_4^+$; 80.7% Ca$^{2+}$; 88.4% Mg$^{2+}$ | [82] |
| MFI-type zeolite | Feed: 0.1 M NaCl; 100 ppm of pantothenic acid; 100 ppm of toluene; 100 ppm of ethanol; 2.76 MPa; 20°C | Rejection 99.4% Na$^+$; flux: 0.35 kg/m$^2$ h; 96.5% rejection; flux: with 0.33 L/m$^2$ h; 99.5% toluene and 17% ethanol rejections with flux 0.03 kg/m$^2$ h | [86] |
| Hydroxysodalite (HS) zeolite | Feed: hydrated ions of size 0.26 nm–0.86 nm; flow rate: 3 L/min; temperature: 60°C; TMP: 3 bars | Water flux: 4 L/m$^2$ h | [84] |
| NaX nano-zeolite/PA | Feed: 2,000 ppm of NaCl and MgSO$_4$; TMP: 12 bar; temperature: 25°C | 29.76 L/m$^2$ h water flux | [85] |
| Polysulfone (PSf) UF/ specific zeolite 4° | Feed: 1,000 mg/L; BSA and pepsin aqueous solutions; TMP: 0.1 MPa | 500 L/m$^2$ h of water flux; rejections 97.0% BSA; 88.6% pepsin | [88] |
| 3% NaA zeolite/UF poly(phthalazinone ether sulfone ketone) | 100 mg/L of polyethylene glycol (PEG) and Titan Yellow dye solution; 0.1 MPa; ambient temperature | 96.8% PEG 6000 rejection; flux: 246 L/m$^2$ h | [89] |
| NaA zeolite | 570 mL of 10:90 water: ethanol mixture; 70°C; 10 mm Hg | ethanol of around 99.5% concentration; 0.4–1.0 kg/m$^2$ h of water flux | [90] |
| Zeolite from natural clinoptilolite | Synthetic seawater with 100 mg/L Na$^+$; 75°C; 1 atm pressure | 99.99%, 98.52%, 97.5% and 97.5% rejection of Mg$^{2+}$, Ca$^{2+}$, Na$^+$ and K$^+$, respectively; 2.5 kg/m$^2$ h water flux | [91] |
| NaA zeolite/PA | 2,000 ppm aqueous solution of PEG; 2,000 ppm aqueous solutions of NaCl and MgSO$_4$; 20°C; 1.24 MPa | 93.9 ± 0.3 NaCl rejection | [92] |

within the PA layer thin-film nanocomposite (TFN) gives higher water fluxes compared to the pristine PA membranes, keeping similar salt rejections [78]. Huang et al. [94] compared two membranes prepared with silicalite-1 and zeolite 4A. The results showed much higher flux for the membranes prepared with silicalite-1 compared to the one prepared with zeolite 4A while both maintained high salt rejection. With those contradicting references, even though some studies reported very high fluxes, the permeability of zeolite membranes still poses a challenge for future emerging desalination applications [97].

Though the improvement of zeolite membranes has been tremendous in the past 10 y, their performance and economics are still worse compared to polymeric membranes. The zeolite membrane thickness is still at least 3 times higher than the current polymeric RO membranes, causing higher resistance to water flux. Consequently, ceramic membranes require at least 50 times higher membrane area than polymeric ones to achieve an equivalent production capacity. This value can be even higher when the higher density and lower packing effectiveness are considered. Moreover, whilst zeolite membranes are claimed to have high organic rejection, organic fouling has caused almost 25% loss in flux after only 2 h of operation, though full recovery of flux was achieved after chemical washing [84].

### 4.2. Membranes based on carbon-nanomaterials

CNT [64,65,98] and graphene-based nanomaterials [66,68], that is, nanoporous graphene (NPG) [66,68,99,100] and GO [101,102] are novel nanomaterials with high potential in the development of membranes, especially in desalination. The main properties of membranes made of these nanomaterials are the following [15,103,104]:

- Unique water transport rate through films containing CNT, NPG and GO.
- High chemical, thermal and mechanical resistance.
- High conductivity, low density and specific optical properties.
- Retention properties are strongly dependent on size of channels to water transport as well as on chemical modifications (e.g., presence of functional groups).

There are two categories of desalination membranes made of CNT, NPG and GO [15]:

- Freestanding CNT, GO or NPG membranes,
- Polymeric membranes modified with CNT, GO or NPG.

In the first group, nanomaterial is directly used as a separation layer, while in the second surface or matrix of polymeric membranes are modified by nanomaterial.

### 4.2.1. Freestanding CNT membranes

Two main types of CNT freestanding membranes may be distinguished, that is, isoporous and "buckypaper" ones [105].

Isoporous membranes are formed from adjusted cylindrical pores in an impermeable matrix, and the flow of liquids takes place only through empty CNTs. They have the fluid flux 2–3 orders of magnitude higher than the one resulted from the fluids flow theory [13]. Vertically oriented CNTs (VA-CNTs) have been introduced to polymeric foil forming nanoporous membrane structure, what has been confirmed by scanning electron microscopy (SEM) images, gas permeation and investigations on the transport of ions [13]. Fig. 6 presents the SEM image and schematic illustration of the structure of an aligned CNT membrane [106]. Water transport and salt retention using VA-CNTs membranes depend mainly on the diameter and homogeneity of CNTs [107,108]. It was stated that by increasing the CNT diameter from 0.66 to 0.93 nm, the ion retention decreases from 100% to 95% [109]. Other studies have shown that by reducing the CNT radius from 0.34 to 0.39 nm, we obtained complete retention of sodium and chloride ions, but water transport inside the CNT takes place without obstacles [110]. Narrower nanotubes have a lower flux and there are difficult to produce membranes for applications in the RO process [111]. Therefore, studies are being carried out on the preparation of VA-CNTs membranes with a diameter of 0.6–0.8 nm with a high water flux at simultaneously maximum ion retention [111].

It has been shown that CNTs functionalization with carboxyl or amine groups on CNTs rims or tips prevents the entering of ions [110], but simultaneously give a slight decrease in the water flux [109]. Holt et al. [103] have examined isoporous CNT membranes of pore size 2 nm and they have stated that water flux is three orders of magnitude higher than the value predicted by the hydrodynamic model. Similar, water permeability through isoporous CNT membranes has been several order of magnitude higher than commercial membranes despite the pore size has been the order of magnitude smaller, which increases selectivity and flux of these membranes [103]. Hummer et al. [112] have shown that the chain of water molecules may permeate fast, frictionless through CNT, what results from hydrogen bonds present in water molecules chain, which are introduced to the hydrophobic interior of CNT, while interactions between carbon and water molecules occurring inside CNT are insignificant. In addition to the higher flux rate and high removal of various salts, VA-CNT membranes exhibit strong antibacterial properties. Brady-Estévez et al. [113] proposed a single-walled carbon nanotube (SWCNT) filter for the removal of pathogen microbes from water, which showed high antibacterial activity for *Escherichia coli* K12 (*E. coli*).

CNT membranes of "buckypaper" type (BP) may be described as randomly distributed CNTs in a non-woven structure similar to paper [105]. The main advantages of such CNT membranes are the presence of a very large porous 3D net and large specific surface. They are prepared using vacuum filtration [114], layer-by-layer (LbL) [115] or electrospinning [116] methods. Peng et al. [114] have formed freestanding CNT membranes using vacuum filtration of suspension of oxidized SWCNTs through a polycarbonate membrane (Fig. 7). After immersion in ethanol ultrathin films have been removed from polycarbonate (PC) support. The obtained CNT membranes have had a thickness of several dozens to several hundred nanometers. The authors suggest, that freestanding CNT films with well-defined nanostructure may potentially be widely used in membrane separation, sensors and catalysis [114].

In Table 4 selected results obtained of water desalination using both SWCNTs and multi-walled carbon nanotubes (MWCNTs), have been presented.

It is worth mentioning that despite the high rate of fluid transport through the VA-CNTs membranes, CNTs alignment control in the matrix over a large area and control of CNTs agglomerations is still a huge challenge. Therefore, future research and development are necessary to verify the feasibility and practicality of VA-CNT membranes in industrial use. The development of a selective membrane with high flux and anti-fouling properties is expected in the future for applications in water and wastewater technology [123].

Despite many advantageous features, BP-CNT membranes after long terms exploitation reveal a significant decrease of water flux as well as delamination due to microcracks initiated by removal of water by capillary forces. This issue may be minimized by the development of methods of CNTs chemical modification, which includes: UV/ozone treatment used to form active hydroxyl an carboxyl sites and coating with a thin PTFE layer [124]. Such actions lead to the improvement in membranes' flux, due to higher hydrophilicity of the materials, and elongate their lifespan.

### 4.2.2. Freestanding GO/NPG membranes

Freestanding membranes made of graphene and graphene oxide are a set of nanosheets, arranged in a series of layers, packed and situated one on another and properly distanced from each other [125]. Water molecules are transported through neighbor hooding nanochannels, while salts are retained (Fig. 8). The effective thickness of one nanosheet of GO/NPG is 0.5 nm, while the site thickness may vary from hundreds of nanometres to dozens of micrometers [102]. Freestanding GO/NPG membranes are flexible and mechanically stable [125,126].

The most important methods of preparation of freestanding GO/NPG membranes are filtration, self-assembly LbL, spray or spin coating, GO/NPG nanosheets casting or an electric field-induced method [101,126,127–129].

The filtration method comprises the creating of GO/NPG layer on the porous membrane (usually UF or MF) at pressure or vacuum and next drying [130,131]. Membranes obtained by means of this method have a thickness from several nanometers to several microns, but the

Table 4
Results of the use of CNT membranes in water desalination

| Material | Feed | Efficiency | References |
|---|---|---|---|
| CNTs-nanolayer Cu | Salt water | Improving selectivity with an increase of the amount of CNTs in the composite | [117] |
| Carboxylated CNTs | NaCl solution of concentration 3.4% | Stability of membrane over a long period of time Water flux: 19.2 kg/m² h | [118] |
| MWCNTs | Solution KCl | Retention mechanism: electrostatic interactions between membrane and ion charge | [119] |
| CNTs | Salt water | CNTs increase porosity and hydrophilicity of the surface and its permeability | [120] |
| Zwitterionic CNTs | Salt water | High water flux and salt retention High resistance to biofouling | [121] |
| MWCNTs oxidized with $HNO_3$ and $H_2SO_4$ | Salt water | Maximum retention was at the highest concentration of salt in raw water | [122] |
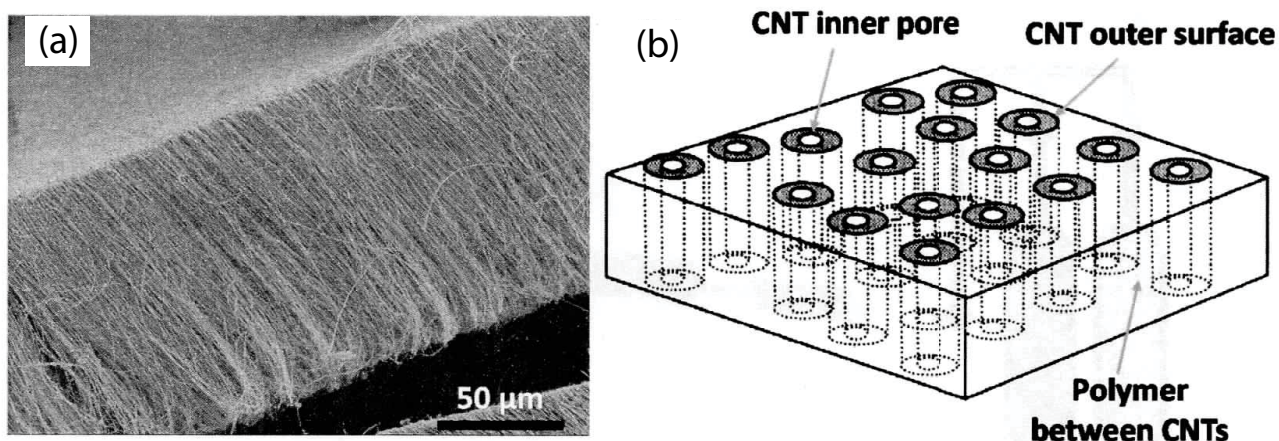


Fig. 6. (a) Scanning electron microscopy (SEM) image of a vertically aligned array of CNTs produced using a Fe-catalysed chemical vapor deposition (CVD) process and (b) schematic illustration of the structure of an aligned CNT membrane [13,106].
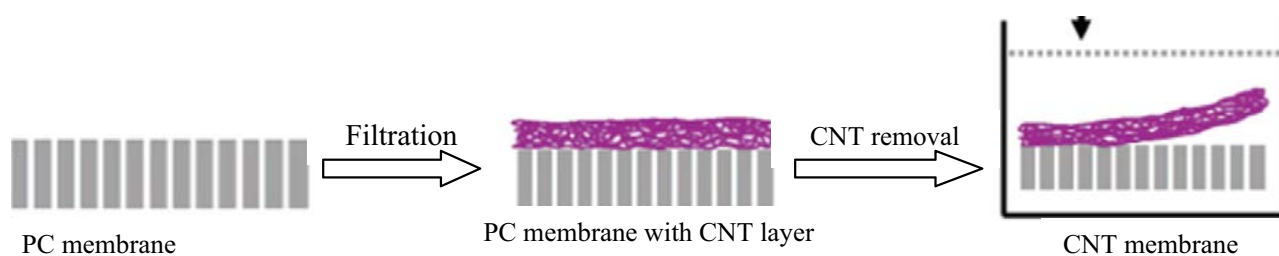


Fig. 7. Preparation of freestanding "buckypaper" type CNT membrane.

connection between neighbor layers is weak and the stability of a membrane is poor.

Nair et al. [126] using a spray or spin coating method from stable dispersion of GO/NPG in water. The obtained membranes have distances between GO/NPG 1 nm and have been completely impermeable to gases, vapors and liquids, except for the permeation of water. The permeability of water through the membrane is, similarly to VA-CNT, due to almost frictionless flow of monolayer of water through 2-D capillaries between graphene sheets placed in the close distance one from another [126]. Hydroxyl and epoxide functional groups attached to GO/NPG nanosheets are also responsible for keeping distance between nanosheets [132].

LbL self-assembly membranes are multilayered nano-architectures obtained by depositing oppositely charged polyelectrolytes or molecules presenting mutually
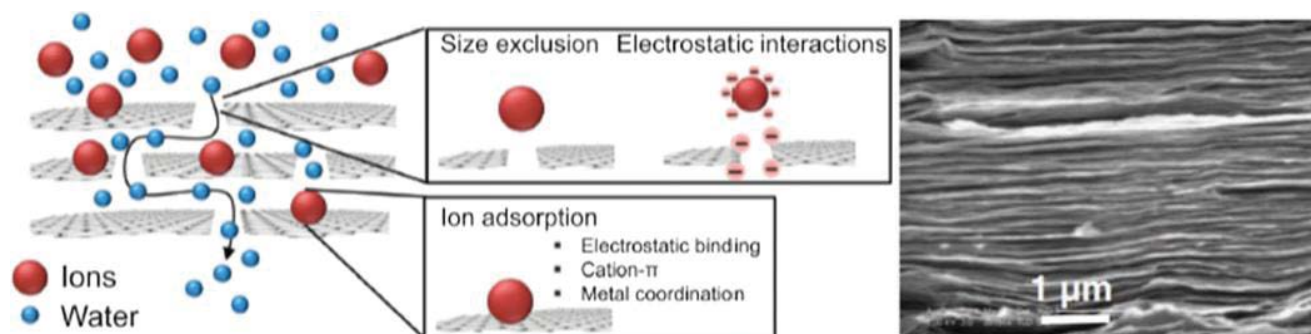
Fig. 8. Scheme of transport mechanisms and SEM image of graphene oxide freestanding membrane ([127]; https://commons.wikimedia.org/wiki/File:Graphite-sheet-side-3D-balls.png).

interacting binding sites [133,134] (Fig. 9). The principal idea of the method consists of the resaturation of poly-ion adsorption, resulting in the alternation of the terminal charge after every subsequent layer deposition. The LbL method can not only be applied to polymers but also to the combinations of polymers with particles. The sequential adsorption of charged polymers and/or nanoparticles is a valuable technique for the formation of thin multilayers.

Permeability of water in freestanding GO/NPG membranes depends on pore size and distance between sheets. Water flux and selectivity of GO/NPG membrane depends also on interlayer nanostructure [135], that is, the increase of porosity and surface of edges of nanosheets may influence of higher permeability of freestanding GO/NPG membranes. The action of OH• radicals on GO/NPG sheets eliminate carbon atoms at edges (as $CO_2$) and inside GO sheet (as CO) and lace-like edges and nanopores on the membrane surface are formed [136]. The elongation of distances between GO/NPG sheets can be partially prevented by the thickening of films, which allows application in desalination, that is, filtration of hydrated ions of smaller radius. The distances between GO sheets should be shorter than 0.7 nm in order to reject hydrated $Na^+$ ions [102]. Mi [137] has stated that distances between nanosheets can be also decreased by chemical reduction of GO or by covalent binding of small particles to GO sheets, which allows for overcoming of hydration forces. For example, GO membrane after carboxylation with glycine (GO-COOH) shows higher permeability and salt retention, because negative GO-COOH surface favors electrostatic repulsion, which characterizes with increase hydrophilicity and a higher number of channels for water transport [138].

Freestanding membranes made of GO/NPG can be used in the water desalination process [139] because they completely rejecting salt, and water flux can be twice as large as commercial RO membranes due to the very low thickness of GO membrane (ca. 10 nm). Cohen-Tanugi and Grossman [140] have stated that the graphene layer with nanopores of diameter below 0.55 nm is suitable for water desalination and retention of salt is higher than commercial RO membranes. They have also stated that water flux through GO freestanding with thickness 10 nm is as high as 400 L/m² d MPa, that is, several times higher than in case of commercial RO membranes. On the other hand, Han et al. [141] have stated that nanofiltration (NF) GO membranes characterize low water flux of 21.8 L/m²h and only 40% salt retention. They explained the reason for poor retention of the presence of open cracks, the appearance of which has been related to GO sheets preparation. Also, Hu and Mi [102] obtained low retention of salt, which was varied from 6%–46%, during their research with the use of graphene membrane, but it water flux was high, that is, in the range of 80 to 276 L/m² h MPa in dependence of a number of GO nanosheets. However, the presence of NaCl and $Na_2SO_4$ can reduce the distances between the GO layer, due to solution ionic strength (ca. 1–2 nm at 100 mM), and due to their hydration and impact of the charge, which compresses
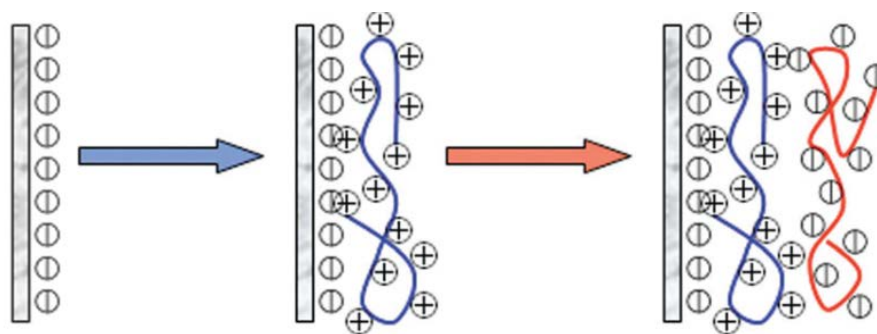


Fig. 9. Schematic of layer-by-layer (LbL) self-assembly of a multilayer coating by sequential adsorption of oppositely charged layers [134].

the electric layer, what often allows for transport of $K^+$ and $Na^+$ disabling its use to water desalination [142].

Xu et al. [143] have used a vacuum filtration technique to form $GO/TiO_2$ membranes by the introduction of $TiO_2$ nanoparticles between GO nanosheets. The presence of functional groups enables easy dispersion of GO nanosheets in water, and thanks to this diameter of the average pores of the prepared membrane have been equal to 3.5 nm. $TiO_2$ nanoparticles interact with GO nanosheets what increases the distance between nanosheets and grows channels for water transport through the membrane. $GO-TiO_2$ nanofiltration membranes have been characterized with complete retention of methyl and rhodamine B what confirms their usability to remove not only hardness but also dyes from water.

In Table 5 exemplary characteristics and efficiencies of freestanding GO/NPG membranes are presented.

Graphene and GO membranes have many advantages over other membranes and that is why they can be used for water desalination. The first and the most important advantage is one atom thickness of NPG/GO sheets and yet mechanical high strength and these two attributes lead to low-pressure requirements and faster water transport. However, experimental data suggest, that multilayer GO/NPG membranes and also CNTs are rather unstable and do not assure sufficient retention of salts and low molecular weight compounds [127,148,149]. Hence, a number of researches on the preparation of hybrid membranes based on carbon nanomaterials combined with polymers are carried out.

### 4.2.3. Composite GO/NPG/CNT membranes

A modification of polymeric/inorganic membranes may be made by the introduction of a nanomaterial either on a membrane's surface or to casting solution followed by membrane formation from the mixture of a polymer and a nanomaterial [127,148–151].

Modification of a polymer surface is performed by interfacial polymerization with the TFC membrane surface resulting in the formation of the TFN membrane [150]

or direct introduction of nanomaterial by means of layer-by-layer method or vacuum filtration [101]. Preparation of membranes by the introduction of nanomaterial on the membrane surface by means of covalent [152], electrostatic [153] or coordination bonding in order to increase separation efficiency may also be applied.

Modification of polymeric or ceramic membrane surface using graphene and its derivatives may improve membrane properties, including antifouling and antibacterial ones [154]. Additionally, membranes with the modified surface are more resistant to chlorine, while the effectiveness of the membrane process is maintained. Modification of membrane surface requires a relatively low amount of nanomaterial, which is economically beneficial and limits the impact of nanomaterial production on the environment.

#### 4.2.3.1. Surface modification with NPG/GO nanoparticles

One of the most commonly used methods for the introduction of CNT/NPG/GO nanoparticles onto polymer membranes surface is interfacial polymerization (IP) [101,155–157]. Initial concentration (IC) occurs at the interface between two immiscible phases (generally two liquids), resulting in a polymer that is constrained to the interface. There are several variations of IP, which result in several types of polymer topologies, but in membrane preparation, the most important is ultra-thin film formation [147,158] have synthesized TFC membrane from GO by IP of *m*-phenylenediamine and 1,3,5-benzenetricarboxyl acid to evaluate its desalination efficiency. The obtained salt retention has reached more than 97% during desalination of the solution of salt concentration 2,000 mg/L at water flux 29.6 $L/m^2$ h and process pressure 1.5 MPa. GO introduction has improved both, membrane stability and antifouling properties.

Yin et al. [159] have introduced GO nanosheets into TFN RO membrane by in situ IP method. With the increase of GO in the membrane from 0 to 0.015 %wt., the permeate flux increased from 39.0 to 60.0 ± 0.4 $L/m^2$ h at 300 psi. NaCl and $Na_2SO_4$ rejection slightly decreased from 95.7% ± 0.6% to 93.8% ± 0.6% and 98.1% ± 0.4% to 97.3% ± 0.3%, respectively.

Table 5
Exemplary characteristics and efficiencies of freestanding GO/NPG membranes

| Preparation method | Membrane type | Process/ conditions | Permeability/ flux | Retention | References |
|---|---|---|---|---|---|
| LbL | GO/PAA/PAN | NF/5 bar | 0.84 $L/m^2$ h bar | 43.2% $Na^+$; 92.6% $Mg^{2+}$ | [144] |
| LbL | GO/PSf | NF/3.4 bar | 27.6 $L/m^2$ h bar | 46% $Na_2SO_4$; 93%–95% rhodamine | [102] |
| Self-assembly | GO-COOH | NF/1.5 MPa | – | 48.2% NaCl; 91.3% $Na_2SO_4$ | [138] |
| Vacuum filtration | GO-PAN nanofibres | NF/1–3 bar | 2 $L/m^2$ h bar | 56.7% $Na_2SO_4$; 100% Congo red | [101] |
| Vacuum filtration | GO with various supports | NF/5 bar | 21.8 $L/m^2$ h bar | >99% dyes; ~20%–60% salts | [145] |
| Vacuum filtration | GO/PVDF | UF | 80–100 $L/m^2$ h bar | Natural organic matter (NOM) | [146] |
| Oxygen plasma etching | Nanoporous single layer graphene | RO/17 kPa | 106 $g/m^2$ s | ~100% monovalent ions | [147] |

PAA – polyallylamine; PAN – polyacrylonitrile; PSf – polysulfone; PVDF – polyvinylidene fluoride.

Xu et al. [160] have made membranes by vacuum filtration of GO suspension through aluminum oxide support coated with polydopamine and then burned in order to improve connection with support and increase the stability of the membrane. The finally obtained membranes have revealed high water flux equal 48.4 L/m² h at NaCl retention 99.7% and temperature 90°C. Similarly, Wang et al. [101] have prepared membranes containing GO on a support made of polyacrylonitrile nanofibers using vacuum filtration of GO suspension. The obtained membranes have moderate retention of bivalent ions equal 56.7% for Na$_2$SO$_4$ with water permeability of 2 L/m² h bar and additionally high retention of dyes (ca. 100% of Congo red). Hu and Mi [102] have used GO crosslinking by using 1,3,5-benzenetricarbonyl chloride (TMC) to covalently bond GO nanosheets on polysulfone (PSf) support coated with polydopamine. The obtained GO membrane has been characterized with water permeability equal from 8 to 27.6 L/m² h bar at relatively low retention of mono- and bivalent ions (6%–46%) and high retention of dyes (93%–95%). What is more interesting, the permeability of water and retention of salts have not changed with the increased number of GO layers. The authors have explained this unique phenomenon by frictionless transport of water between the GO layer.

GO with carboxylic, hydroxyl, epoxide and amide groups may be used for the preparation of desalination membranes using the self-assembly LbL method. Carboxylic and amine groups on GO surface formed negative charge of GO particles dispersed in water, thus they can move in an electric field, during the formation of self-assembly film. Kim et al. [161], using the LbL method, have coated polyethersulphone (PES) membrane surface with negatively charged GO nanoparticles and the next deposited positively charged GO layer with amine groups on the negative layer. The modified membrane has revealed high water flux equal to 28 L/m² h and 98% retention of salt. Choi et al. [153] have also used the LbL technique to modify the PA membrane surface with GO and amine-functionalized GO (aGO) nanosheets. The modified membrane has shown good resistance to chlorine degradation and to fouling and has shown a 10% flux increase, while NaCl retention measured during filtration of a water solution containing 2,000 mg/L of salt has decreased by 0.7%.

Covalent bonding may be used to the modifier of desalination membranes surface with GO. For example, an amide bond can be formed between carboxylic groups attached to GO nanosheets with other carboxylic groups present on the thin polyamide layer (PA) of the TFC membrane (Fig. 10) [152]. Functionalization of the PA surface in TFC membranes causes that nanosheets are better arranged of the membrane surface, which has a positive effect on antibacterial and hydrophilic properties of modified membranes. It has been found that surface hydrophilicity does not increase membrane water flux, as water flux is regulated by the solution–diffusion mechanism in the active PA layer (TFC), independently of surface modification [40].

One of the main issues in membrane exploitation to desalination is fouling, which significantly depends on membrane material selection, chemical features of its surface and structure porosity [162]. NPG and GO can improve resistance to fouling because they reveal the ability to inactivate bacteria in direct contact with their cells [152,154,162–165]. Perreault et al. [152] have investigated the impact of LbL modification of membrane with GO to improve the antibacterial properties of TFC membranes made of PA. It has been shown that 65% of *E. coli* cells become deactivated during direct contact with the membrane within 1 h. It has been found that GO deactivates bacteria by the initiation of physical damage of the cell's membrane [154] followed by the eventual extraction of lipids out of the cell [153]. SEM images show that cells, which are in contact with the GO membrane seem to be flattened or shrunken in comparison with cells observed on the reference membrane. Such the antibacterial behavior of the modified membrane does not cause any losses in its transport properties.

Antibacterial and anti-biofouling properties of TFC membranes can be also improved by an introduction to membrane surface the metal nanoparticles. Sun et al. [164] have presented research describing the preparation of composite membranes made of cellulose acetate (CA) modified with graphene containing silver nanoparticles (GO-AgNP). The decrease of relative permeate flux of composite GO-AgNP membrane has reached 46%, that is, much less than in case of CA reference membranes (88%). Additionally, the flux of the composite GO-AgNP membrane is higher than one measured for membranes modified only with GO or only with AgNP. Composite GO-AgNP membranes efficiently prevent bacteria growth and formation of biofilm on the membrane surface causing 86% *E. coli* inactivation after 2 h contact the membrane. Ma et al. [165] have introduced copper nanoparticles (CuNPs) on the polyamide RO membrane in order to decrease its biofouling.

In Table 6, the list of selected surface-modified membranes with GO/NPG is given together with their characteristics.

### 4.2.3.2. Surface modification with CNT nanoparticles

Due to difficulties related to the preparation of membranes containing vertically oriented CNT, which characterize by proper retention of solutes, many researchers
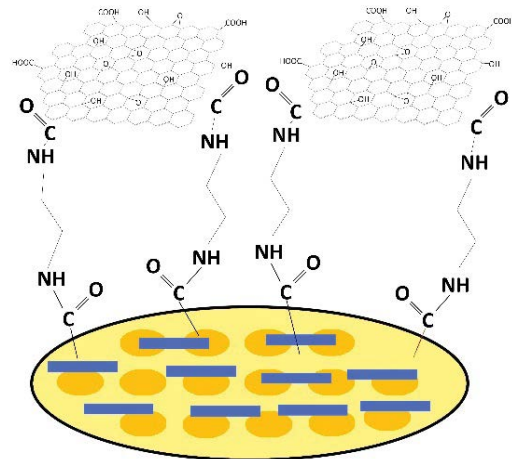
Fig. 10. The scheme of modification of the membrane surface by covalent bonding.

Table 6
Selected results of researches on surface modification of polymeric membranes using GO/NPG

| Preparation method | Base polymer | Membrane process/pressure | Permeability/flux | Retention+ | References |
|---|---|---|---|---|---|
| IP | GO/PA | RO – 15 bar | 29.6 L/m² h | >97% NaCl | [147] |
| IP | GO/PA | NF – 8 bar | 353.5 L/m² h bar | 59.5% NaCl; 95.2% Na₂SO₄; 91.1% MgSO₄; 62.1% MgCl₂ | [166] |
| IP | GO/PA | NF | 22 L/m² h | >88% NaCl; >97%MgSO₄ | [167] |
| IP | GO/polypiperazine-amide | NF – 0.6 MPa | 87.6 L/m² h | 56.8% NaCl; 98.2% Na₂SO₄; 96.5% MgSO₄; 50.5% MgCl₂ | [101] |
| IP | rGO/TiO₂/PSf | NF – 10 bar | 60.6 L/m² h | 36.6 NaCl; 93.6 Na₂SO₄ | [168] |
| IP | rGO/TiO₂ (0.2% wt.)/PA | RO – 15 bar | 3.42 l/m² h bar | 99.45% NaCl | [169] |
| LbL | GO-PA | RO – 15.5 bar | 0.9 L/m² h bar | 96.4% NaCl | [153] |
| Self-assembly LbL | GO-chitosan/PSf | NF | 1.78 L/m² h bar | 62% NaCl; 92.7% Na₂SO₄ | [170] |
| Coating LbL | aGO/GO/aPES | RO – 5,500 kPa | 28 L/m² h | 98% NaCl | [170] |
| Coating | PSf-GO (0.3% wt.) | NF – 0.6 MPa | 2.45 L/m² h bar | 59.5 NaCl; 95.2 Na₂SO₄ | [166] |
| Coating | GO-PSf | NF – 10 bar | 5.47 L/m² h bar | 33% NaCl; 89.8% Na₂SO₄ | [168] |
| Coordinate bond | *f*-GO-PA | RO – 27.6 bar | Ab.1.45 L/m² h bar | 97.8% NaCl | [152] |
| Vacuum filtration | GO/PAN | NF – 1.0 bar | 8.2 L/m² h bar | 9.8% NaCl; 56.7% Na₂SO₄ | [101] |
| Vacuum filtration | rGO-CNT-AAO | NF | 31.5 L/m² h bar | 42% NaCl; 84% Na₂SO₄ | [171] |

IP – interfacial polymerization; LbL – layer-by-layer; CNT – carbon nanotube; PA – polyamide; rGO – reduced graphene oxide; *f*-GO – functionalized graphene oxide; PES – polyethersulphone; aPES – aminated polyethersulphone; PSf - polysulfone; PAN – polyacrylonitrile; AAO – anodic aluminum oxide.

have focused on the preparation of TFN membranes based on CNT, in which CNT are introduced to the retention layer [172]. As CNT are hydrophobic and non-reactive, which often causes incompatibility with polymeric matrices, a number of methods of chemical or physical modification have been developed to improve CNT dispersion in a coating solution [173]. Among them the use of acid is found to be the most efficient method as it allows to form hydroxyl (–OH) and carboxylic (–COOH) groups at CNT ends making them more hydrophilic and more reactive [174]. Functionalized CNT may be next introduced to a thin skin layer made of polyamide [174], which may significantly influence on physicochemical properties of membranes (e.g., hydrophilicity, porosity, charge density and additional water channels) [175]. A number of research has also shown that TFN membranes based on CNT characterize improved antifouling properties [149] as CNT possesses strong antibacterial properties.

Fig. 11 presents a scheme of RO membrane obtained with conventional IP on polymeric microporous support. The open ends of CNTs with a diameter of approximately 0.8 nm are embedded on a selective layer, with the thickness of the active layer being much less than the average length of CNTs, allowing nanotubes to be randomly oriented to the matrix and the channels extending through the layer allow for selective water permeation, at a rate almost twice as high as membranes not containing CNTs with a slight increase in salt retention [176].

Polyamide RO membranes with CNTs are frequently prepared by IP method using trimesoyl chloride (TMC) solutions in *n*-hexane and aqueous solutions of *m*-phenylenediamine (MPD) containing functionalized CNTs with an acid mixture of sulfuric and nitric acids) [177,178]. It was shown that with an increase in the carbon nanotube loading in the membrane, the membrane morphology changed distinctly, leading to a significantly improved flux without sacrificing the solute rejection, and the surface of the nanocomposite membrane was more negatively charged than the pristine polyamide membrane. Furthermore, the durability and chemical resistance against NaCl solutions of the membranes containing CNTs are found to be improved compared with those of the membrane without CNTs. The nanocomposite membranes showed better antifouling and antioxidative properties than MWCNT-free polyamide membranes, suggesting that the incorporation of modified MWCNTs in membranes is effective for improving membrane performance.

Xue et al. [172] have functionalized MWCNTs with three different functional groups, that is, carboxylic (MWCNT-COOH), hydroxyl (MWCNT-OH) and amine (MWCNT-NH$_2$) ones, and next they have introduced functionalized CNT to an aqueous solution of piperazine (PIP) in order to prepare TFN membranes via IP method. At the optimum concentration of 0.01% (m/v) of MWCNT, all membranes have revealed higher permeability of pure water and higher retention of salts. Among three types of MWCNTs membranes, the TFN MWCNT-OH membrane has revealed the highest water flux and salt retention. The authors have related this capacity to the synergy of –OH groups in MWCNTs and –NH$_2$ groups in PIP. Additionally, membranes with MWCNTs-NH$_2$ have revealed better salt retention and stability than MWCNT-COOH due to adhesion between –NH$_2$ and –COOH in PA matrix.

Chan et al. [121] have introduced positively and negatively charged CNT using vacuum filtration to produce high-quality RO membranes. The obtained CNT containing membranes has been characterized with four times higher water permeability (1.3 L/m$^2$ h bar for TFN vs. 0.3 L/m$^2$ h bar for TFC) and retention almost identical to non-modified membranes (98.6% for TFN vs 97.6% for TFC). The authors have related increased permeability of the modified membrane to ultrafast transport through CNT, which has been uniformly distributed on the ultrathin skin layer.

Tiraferri et al. [179] have presented the new strategy for the immobilization of CNTs functionalized with a carboxylic group on the skin layer of the polyamide membrane, which involves strong covalent bonding (Fig. 12). Before modification, CNTs had been functionalized with carboxylic groups and next 1-ethyl-3-(3-dimethylaminopropyl) carbodiimide (EDC/NHS) solution has been used to transform carboxylic groups of polyamide thin layer to semi-stable amino-reactive in order to enable reaction with ethylenediamine (ED). Characterization of the SWCNT-functionalized surfaces demonstrated the attainment of membranes with novel properties that continued to exhibit high performance in water separation processes. The presence of surface-bound antimicrobial single-walled carbon naotubes (SWCNTs) was confirmed by experiments using *E. coli* cells that demonstrated enhanced bacterial cytotoxicity for the SWCNT-coated membranes. The SWCNT membranes were observed to achieve up to 60% inactivation of bacteria attached to the membrane within 1 h of contact time. Our results suggest the potential of covalently bonded SWCNTs to delay the onset of membrane biofouling during operation.
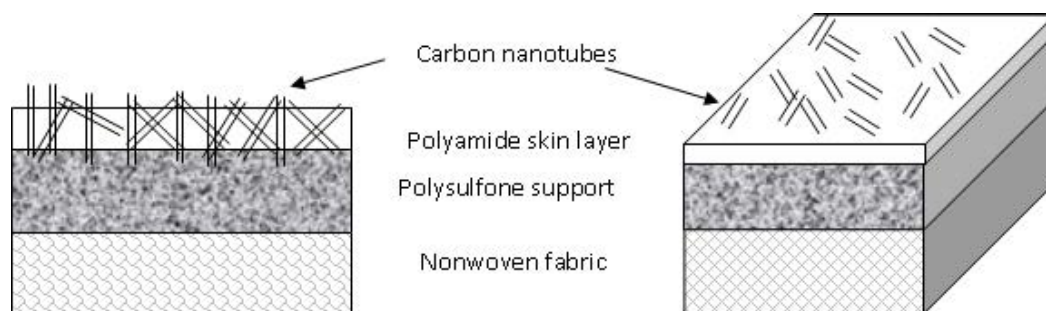


Fig. 11. Cross-section diagram of the TFC membrane containing CNTs in the active layer.
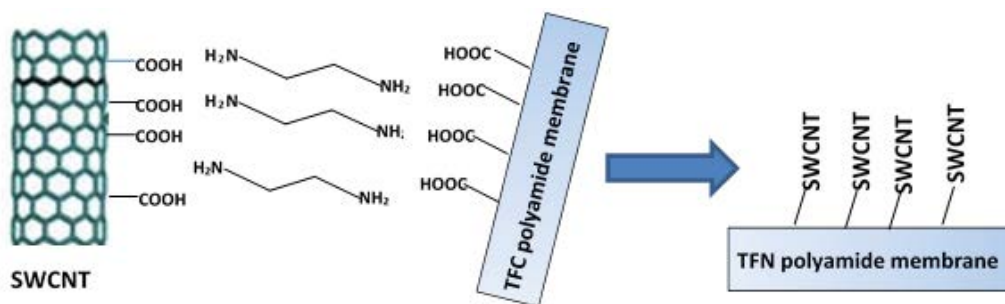
Fig. 12. The scheme of CNT immobilization on the PA TFC membrane.

Zhang et al. [180] have connected GO with oxidized CNT to modify the PVDF membrane. The presence of long and curled CNT allows us to prevent GO aggregation, as they reveal the tendency to bind with neighbor hooding GO nanosheets. Modified GO-CNT membrane has shown much higher hydrophilicity and antifouling properties than membranes modified only with GO or only with CNT. Water flux of membranes modified with GO and CNT in weight ratio equal 1:1 has been increased by 252% in comparison with the PVDF reference membrane.

### 4.2.3.3. Modification of membrane matrix

Membranes made of polymeric materials, as aromatic and aliphatic polyamides, cellulose acetate, PVDF, polysulfone, sulfonated polyether and non-polymeric materials (ceramic, metals) and their composites are used in desalination [181,182]. The introduction of carbon nanomaterials to polymeric membrane matrix influences its structure and antibacterial properties as well as hydrophilicity, water permeation, retention and mechanical strength [180,183–185]. In comparison with conventional membranes, the surface of the modified membrane characterized by a dense pore structure, which is the result of nanomaterial precipitation during the phase inversion process. Hence, the introduction of carbon nanomaterials enables exploitation in a dry state without permeability affection, which is especially important to the resistance of microorganisms and enhances transport.

The most commonly used method of introducing carbon nanomaterials into the polymer membrane matrix is the phase inversion process [186–190]. Phase inversion is a process of controlled polymer transformation from a liquid phase to a solid phase. There are four basic techniques used to create phase inversion membranes: precipitation from the vapor phase, precipitation by controlled evaporation, thermally induced phase separation, and immersion precipitation (Fig. 13).

Out of the four, immersion precipitation is the most widely-used technique for preparing polymeric membranes. In comparison with conventional membranes (without nanomaterial), the surface of the modified membrane is characterized by a dense pore structure, which is the result of nanomaterial precipitation during the phase inversion process. The significant increase of membrane hydrophilicity results in increased water permeation of the modified membrane. Hence, the introduction of carbon nanomaterials creates the opportunity for membranes exploitation in a dry state without permeability affection, which is especially important in regard to membrane resistance to microorganisms and enhances transport.

Wet phase inversion method is used to prepare first of all of ultrafiltration or microfiltration membranes, while dry phase inversion one to nanofiltration and RO membranes.

Lee et al. [184] have explained the role of nanomaterials in the phase inversion process during membrane casting. When GO-CNT is absent, the polymer solution quickly solidifies at the phase boundary between polymer and non-solvent during phase separation due to the concentration gradient and fast interaction of all components. In non-stable parts, polymeric surface damages and scratches can appear due to fast desolvation. The introduction of hydrophilic substances (nanomaterials) to casting solution increases its hydrophilicity and increases the exchange rate between solvent and non-solvent during phase separation, and thus the number of damages and macro-holes are minimized. The obtained membrane structure is more porous, however, the use of small amounts of functionalized nanomaterials
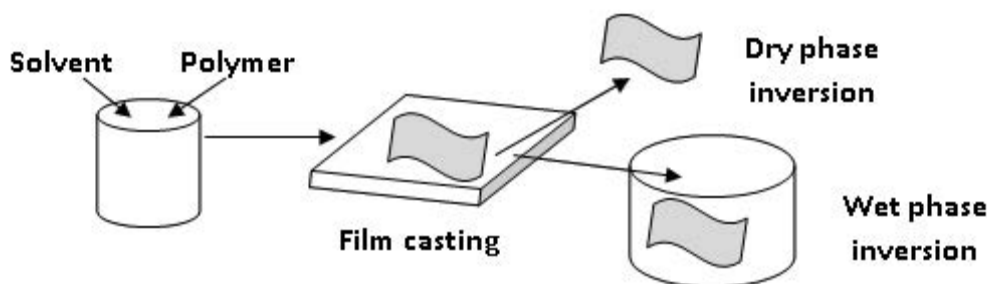


Fig. 13. The idea of polymer membranes preparation using the phase inversion method.

leads to an increase of porosity and membrane pore size, but only to some critical point [186,187]. If the amount of nanomaterial exceeds 0.5%, the porosity of the membrane noticeably decreases [191]. This trend corresponds to permeability test results, which also increases with nanomaterial addition up to a critical point, after exceedance of which it starts to decrease [191]. Xia and Ni [146] have prepared PVDF membranes of different GO content using the phase inversion method, which has significantly improved water transport rate and antifouling properties.

Functionalized nanomaterial, due to the presence of acidic groups, may yield negative charge on membrane surface in the whole pH range [192], which increases the separation of positive ions due to repulsion of negative ions by negatively charged membrane surface. Nanomaterials cause the increase of the membrane hydrophilicity, which increases permeate flux during RO/NF processes because the more hydrophilic membrane has a higher affinity to water molecules in the membrane matrix and enables their permeation through the membrane [193].

The research carried out by Bano et al. [166] have shown the increase of permeate flux and retention of salt caused by non-functionalized GO to PSf support covered with polyamide layer. Membranes prepared with casting solution containing 0.3 wt. % GO have retention of $Na_2SO_4$, $Mg_2SO_4$, $MgCl_2$ and NaCl equal 95.2%, 91.1%, 62.1% and 59.5%, respectively.

Functionalized, hydrophilic nanoparticles mixed with polymeric matrix improve membrane properties [194]. For membrane made of functionalized GO (*f*-GO) the porosity improves due to the formation of more dense pores, but only if a small amount of *f*-GO is added, while if the critical amount is exceeded, the porosity of a membrane decreases [185,195]. *f*-GO introduction also increases thermodynamic instability during the gelling process, which stimulates the phase separation stage, that is, fast exchange of solvent with non-solvent, resulting in the formation of a large number of pores with a small amount of *f*-GO on the membrane surface [185]. When *f*-GO amount is higher than 0.5 wt.%, its coagulation during phase inversion increases the viscosity of the casting solution and membrane porosity is significantly decreased [195]. Additionally, it has been observed that the increase of *f*-GO layers number affects the retention of some metal ions, for example, $Na^+$ and $Mg^{2+}$, while water permeability is simultaneously decreased.

RO or nanofiltration mixed nanocomposite membranes are prepared first of all using the dry phase inversion method. Previous investigators have made polymer–nanomaterial composites by mixing the nanomaterial and polymer in a suitable solvent before evaporating the solvent to form a composite film [196–200]. One of the benefits of this method is that agitation of the nanomaterials added as a powder to the solvent facilitates material de-aggregation and dispersion. Almost all solution-processing methods are variations on a general theme that can be summarized as (i) dispersion of nanomaterial in either a solvent or polymer solution by energetic agitation; (ii) mixing of nanomaterial and polymer in solution; (iii) casting the solution onto a clean surface; (iv) controlled evaporation of the solvent, leaving a composite film. In general, agitation is provided by magnetic stirring, shear mixing, reflux, or, most commonly, ultrasonication.

Mehwish et al. [199] used the dry phase inversion method for the synthesis of silver modified nanocomposite nanofiltration membranes PVDF/poly(styrene-butadiene-styrene)(SBS)/thiocyanate and MWCNTs. The PVDF and SBS mixture has been prepared by dissolving and mixing at room temperature of two polymers (1:1) in tetrahydrofuran. Modified MWCNTs (0.01–0.1 wt.%) have been added to the finished mixture, poured on a glass plate and left to evaporate at room temperature to produce membranes pure water flux, salt rejection, and recovery were found optimal for 0.05% wt. silver nanoparticle-based modified system. Novel membranes have fine nanofiltration characteristics to be utilized in advanced water treatment industrial units.

Shawky et al. [200] have prepared nanocomposite membranes MWCNT/aromatic PA for reverse osmosis with dry phase inversion method using N,N-dimethylacetamide (DMAc) as a solvent. MWCNTs were dispersed in DMAc assisted ultrasonically and then benzoyl peroxide (BPO) was added to enhance dispersion and facilitate to obtain of a more homogeneous MWCNTs-PA mixture. The resulting solution was poured into a dried clean glass plate and placed in a dryer at 90°C for 30 min to evaporate the solvent. The formed uniform thin membrane with a thickness of 200 μm was immediately cooled and immersed in a distilled water bath for at least 15 h at room temperature. The addition of MWCNTs improved the rejection of both salt and organic matter relative to the 10% PA membrane base case. The nanocomposite membrane synthesized with 15 mg/g MWCNT in a 10% PA casting solution rejected NaCl and humic acid by factors of 3.17 and 1.67 respectively relative to the PA membrane without MWCNTs, while membrane permeability decreased by 6.5%.

Table 7 contain selected studies onto the desalination of water by membranes containing *f*-CNT.

### 4.2.3.4. Desalination using diffusion membrane techniques

As noted in paragraph 3, research is being carried out on the introduction of nanoparticles into FO membranes to increase efficiency and reduce internal concentration polarization, both using simulation studies and experimental [201–203]. It has been observed that the introduction into the nanocomposite FO membrane <0.1% MWCNTs (optimum 0.05%), resulted in a 2.5-fold increase in the flux from 35.7 L/m²h for the TFC membrane to 96.7 L/m²h for the TFN membrane. It can be assumed that MWCNTs form nanochannels, which increase water permeability, and functionalization with amine increases membrane hydrophilicity [201].

Goh et al. [203] made polyethyleneimine-poly(amide imide) membranes containing immobilized MWCNT in membrane structure using a vacuum filtration method. FO test results showed that modified membranes reached a flux of 13.4 L/m²h, which was 44% higher than membranes without MWCNT.

Dumée et al. [202] fabricated TFN FO membranes by IP a dense PA layer on self-supporting BPs made of hydroxyl-functionalized CNTs. These hydrophilic supports exhibited low water contact angle (<20°), high water uptake capacity (17 wt.%), large porosity (>90%), making it a promising material, when compared with PSf, used to make TFC membrane supports in RO.

Table 7
List of studies on membrane desalination of water by membranes with *f*-CNT

| Type of salt | Membrane type | CNT membranes | | Matrix | IC | Load of CNTs g/cm² or %wt./cm² | Removal mechanism | Comments | Reference |
| --- | --- | --- | --- | --- | --- | --- | --- | --- | --- |
| | | R (%) | Diameter, nm | | | | | | |
| NaCl | E-CNTs | 99% | N/A | PVDF | 35,000 mg/L | 2 g/9.3 cm² | Chemical interactions | Very high water permeability | [204] |
| | Amine-functionalized MWCNTs | 20% | 5–20 nm | PES | 200 mg/L | 0.045 wt.%/19.6 cm² | Electrostatic interaction Donnan effect | High anti-fouling properties to bovine serum albumin (BSA), flux and NaCl retention | [205] |
| | COOH-MWCNTs | >90% | 5 nm | PSf | 584 mg/L | 2% w/v/18.1 cm² | Electrostatic interaction complexation | High anti-fouling and antioxidant properties | [177] |
| | COOH-MWCNTs | 98.5% | 5–15 nm | Poly-amide | 2,000 mg/L | 0.025%/36 cm² | Surface complexing | High water permeability and BSA antifouling properties | [157] |
| | Oxidized CNTs | >98% | 10–20 nm | PSf | 2,000 mg/L | 0.4 g/3.3 × 68 cm² | Surface complexing, electrostatic interaction | Excellent anti-biofouling properties to dissolved organic matter (DOM) | [178] |
| | Acid modified MWCNTs-nAg | 88.1% | 5–10 nm | PSf | 2,000 mg/L | 5.0 wt.%/0.01764 cm² | Chemical interactions | High permeability, and retention and anti-biofouling abilities | [206] |
| Na₂SO₄ | Sulfonated MWCNT-OH | 96.8% | <8 nm | PES | 1,000 mg/L | 1 g/12.56 cm² | Electro-static interaction/Donnan effect | High antifouling efficiency to NOM | [207] |
| | PMMA–MWCNTs | >99% | 20–30nm | PSf | 2,000 mg/L | 0.67 g/19.62 cm² | N/A | Significantly increased selectivity and permeability | [205] |
| | Amina-functionalized MWCNTs | 65% | 5–20 nm | PES | 200 mg/L | 0.045 %wt./19.6 cm² | Electrostatic interaction/Donnan effect | High permeability and high antifouling properties to BSA, high Na₂SO₄ retention | [208] |
| | *f*-MWCNTs-nAg/TFN | 95.6% | 5–10 nm | PSf | 2,000 mg/L | 5.0 wt.%/0.01764 cm² | Chemical interactions | Anti-biofouling properties. High retention and flux | [206] |
| MgSO₄ | Amine-functionalized MWCNTs | 45% | 5–20 nm | PES | 200 mg/L | 0.045 wt.%/19.6 cm² | Electrostatic interaction/Donnan effect | High water permeability and strong BSA antifouling properties | [205] |

*R* – efficiency of salt removal, %; IC – initial concentration, mg/L; PMMA – poly(methyl methacrylate); N/A represent not available.

Shen et al. [209] GO nanosheets incorporated into the PA selective layer to develop a novel TFC membrane for FO application. The chemical structure and morphology of the synthesized GO and GO-incorporated TFC membranes are studied by various characterization techniques. Compared with the control TFC membrane, GO-incorporated TFC membranes exhibit higher water flux and reasonable draw solute rejection. The effects of the GO loading on the membrane morphology and FO performance of the GO-incorporated TFC membranes are investigated systematically in terms of various characterizations and intrinsic separation performance. The influence of the draw solution concentration is also studied. The GO-incorporated TFC membranes also possess lower fouling propensity in the FO test than that without embedded GO.

A novel PA-GO membrane was synthesized on polyethersulfone support by first intra-crosslinking GO aggregates via *m*-xylylenediamine (MXDA) and then inter-crosslinking GO aggregates via TMC [210]. This method allows for the use of hydrophilic, more porous supports in FO membranes, thereby lending much flexibility to membrane synthesis and also potentially reducing internal concentration polarization in FO. The elemental composition, morphology, and hydrophilicity of the synthesized PA-GO membrane were characterized to confirm intra- and inter-crosslinking reactions and understand membrane properties.

Hung et al. [211] were fabricated FO membranes based on ultrathin GO. Suitable crosslinking agents were used to tune the interlayer spacing of GO sheets to achieve the desired membrane performance. The physicochemical properties of membranes were evaluated using different techniques. The interlayer spacing of GO-based membranes has controlled the interaction between the surface functionality of GO with the nature of crosslinking agents, such as polyvinyl alcohol, MPD and TMC. The covalent bonds between the layer and crosslinking agents effectively suppressed the d-spacing stretching. Unlike other symmetric structures of membranes, the GO-MPD/TMC behavior observed in the ultrathin polyamide (36 nm) asymmetric structure for the performance of pressure-retarded osmosis (PRO) model showed the highest flux of 20.8 LMH and low reverse salt flux of 3.4 g MH. A consistent water flux for a long-term PRO operation was achieved using GO-MPD/TMC membrane (~98.7%). Therefore, the GO-MPD/TMC membrane can be used to suppress internal concentration polarisation.

Suwaileh et al. [212] report the use of a LbL surface modification method to fabricate novel positively charged FO membranes. The main purpose of this work was to fabricate an effective selective layer onto a commercial PES UF membrane, which functioned as a support layer, to provide the best performance for the treatment of brackish water by FO. The new membranes containing a mixing ratio of 0.1 MPDADMAC:0.001 MCMCNa in the polyelectrolyte complex exhibited the best performance in terms of minimum reverse solute flux and acceptable water flux as compared to that for membranes containing a mixing ratio of 0.1 MPDADMAC:0.01 MCMCNa. The improved performance and physicochemical properties of the new membranes were explored by various analytical techniques and were compared to the pristine membrane. Firstly, structural characterization revealed that the new selective layer was homogenous, uniform and strongly adhered to the substrate resulting in excellent water permeability and acceptable reverse solute flux. Secondly, it was found that the optimal curing temperature was 60°C for 4 h that contributed to enhanced membrane performance. Lastly, the developed ranking protocol was adopted to optimize the membrane performance in terms of the water permeability coefficient (*A*) and the solute permeability coefficient (*B*). According to this optimization procedure, the best performing membrane was membrane coated 2.5 bilayers which had water permeability and solute permeability coefficients of 23.1 L m$^{-2}$ h$^{-1}$ bar$^{-1}$ and 1.54 L m$^{-2}$ h$^{-1}$ respectively.

In contrast to other desalination techniques, such as NF and RO, direct contact membrane distillation (DCMD) offers a potentially low energy and high rejection route to the desalination of highly dirty or salty waters. It is consequently important to investigate other alternatives as well as techniques for improving the process efficiency by modifying the membrane properties and structure.

CNT nanocomposite membranes and bucky paper CNT membranes have been found to have high desalination efficiency in MD, as confirmed in laboratory-scale studies [48,188,213].

Dumée et al. [48,124] received BP and CNT composite membranes that they used in the MD process. Self-supporting BP-CNT membranes have been prepared by vacuum filtration through 0.2 μm PES 0.2 μm pore size support followed by flaking of the imposed layer. They have characterized with higher porosity (90%), hydrophobicity (contact angle 113°), heat flux (2.7 kW/m$^2$ h) and salt retention equal 99% and distillate flux 12 kg/m$^2$h (seawater 35 g NaCl/L) in comparison with PTFE membrane. BP membranes had a 20% higher porosity compared to conventional PTFE membranes, but in the MD process, they did not show a higher water flux and salt retention (99%) compared to conventional PTFE membranes [48]. On the other hand, CNT composite membranes have shown greater durability, performance and salt retention compared to freestanding BP membranes.

Bhadra et al. [118] have used MWCNTs functionalized with –COOH groups to the preparation of freestanding CNT membrane dedicated to MD. The use of MWCNTs with carboxylic groups increases polarity and interaction between membrane surface and water vapor, which results in the increase of MD-based desalination. Distillate flux equal 19.2 kg/m$^2$ h measured for the MWCNT membrane is higher than the one obtained for conventional PVDF membranes.

Although the BP made from CNTs possesses beneficial characteristics of hydrophobic nature and high porosity for MD application, the weak mechanical strength of BP has often prevented the stable operation. A study performed by Kim and Lee [214] aims to fabricate BP with high mechanical strength to improve its MD performance. The strategy was to increase the purity level of CNTs with an assumption that purer CNTs would increase the Van der Waals attraction, leading to the improvement of the mechanical strength of BP. According to this study results, the purification of CNT does not necessarily enhance the mechanical strength of BP. The BP made from purer CNTs demonstrated a high flux (142 kg/m$^2$ h) even at low $\Delta T$ (50°C and 20°C)

during the experiments of DCMD. However, the operation was not stable because a crack quickly formed. Then, a support layer of anodic aluminum oxide (AAO) filter paper was introduced to reinforce the mechanical strength of BP. The support reinforcement was able to increase the mechanical strength, but wetting occurred. Therefore, the mixed matrix membrane (PSf-CNT) using CNTs as filler to polysulfone was fabricated. The DCMD operation with the PSf-CNT membrane was stable, although the flux was low (6.1 kg/m$^2$ h). This result suggests that the mixed matrix membrane could be more beneficial for the stable DCMD operation than the BP.

Bhadra et al. [215] demonstrate the immobilization of graphene oxide on PTFE membrane surface for desalination via DCMD. The graphene oxide immobilized membrane significantly enhanced the overall permeate flux with complete salt rejection, and the flux reached as high as 97 kg/m$^2$ h at 80°C. Authors attribute this enhancement in flux to multiple factors including selective sorption, nanocapillary effect, reduced temperature polarization as well as the presence of polar functional groups in graphene oxide.

Athanasekou et al. [216] elucidate the influence of graphene and GO content on the desalination performance and scaling characteristics of graphene/PVDF mixed matrix and GO/PVDF composite-skin membranes, applied in a DCMD process. Inclusion of high quality, nonoxidized, monolayered graphene sheets as polymer membrane filler, and application of a novel GO/water-bath coagulation method for the preparation of the GO/PVDF composite films, took place. Water permeability and desalination tests via DCMD, revealed that the optimal graphene content was 0.87 wt.%. At such concentration, the water vapor flux of the graphene/PVDF membrane was 1.7 times that of the nonmodified reference, while the salt rejection efficiency was significantly improved (99.8%) as compared to the neat PVDF. Similarly, the GO/PVDF surface-modified membrane, prepared using a GO dispersion with a low concentration (0.5 g/L), exhibited twofold higher water vapor permeate flux as compared to the neat PVDF, but however, it is salt rejection efficiency was moderate (80%), probably due to pore wetting during DCMD. The relatively low scaling tendency observed for both graphene and GO modified membranes is primarily attributed to their smoother surface texture as compared to neat PVDF while scaling is caused by the deposition of calcite crystals, identified by XRPD analysis.

Carbon nanomaterials contribute to improving transport and separation properties not only membranes used in RO, FO and MD but have also been used in electrochemical desalination processes, primarily by the CDI method. The literature describes several polymer composite materials that contain CNT or other nanomaterials to increase the conductivity of CDI electrodes, pore-volume, mesoporosity, (pore diameters 5–20 nm), electron-ion sorption, the efficiency of desalination, effective and rapid regeneration of ions and ultimately reduced energy consumption [57,58,217]. Most findings indicate that the addition of CNTs to polymers or other materials forming electrodes based on the nanocarbon structure offers promising opportunities in the CDI process.

Wimalasiri and Zou [217] studied CDI performance using electrodes containing SW-CNT in combination with nanographene sheets. The CNT-graphene composite electrode had more favorable properties compared to electrodes that use only graphene sheets. SWCNTs insert between graphene nanosheets formed diffusion channels that facilitated the transport of ions, increased pore density, formed a mesopore network, increased electrode conductivity, which allowed for high removal efficiency of salts up to 98%.

In another study, Hou et al. [57] have developed MWCNT/poly(vinyl alcohol) composite (MWCNT/PVA) as an electrode for CDI. Results showed that compared to electrodes from activated carbon, SWCNT/PVA composites showed twice the electro-sorption efficiency, had a larger area for efficient ion electro-sorption and reduced energy consumption. Similar improvements of CDI electrodes were made by combining conductive polypyrrole polymer and CNT to form a polypyrrole/CNT composite with increased adsorption capacity compared to CNT itself [218,219] in turn combined polyaniline with SWCNT and observed an improvement of the mesopore volumes and electrochemical properties of the composite compared to polyaniline or SWCNT, and salt removal efficiency increased by 12% compared to SWCNT electrodes.

Li et al. [219] and Liu et al. [220] proposed the introduction of CNTs into polymer ion exchange membranes for use in the CDI process. Ion exchange membranes prevent the attraction of the ions to the electrodes in the regeneration phase. Liu et al. [220] combined CNT electrodes with anionic polymer – dimethyldiallylammonium chloride (DMDAAC) – and cationic polymer polyethyleneimine (PEI) and studied membrane efficiency. The results of the tests in this regard led to an improvement in the mesoporosity and microstructure of the CNT film. Polymer fraction of the ion exchange composite membrane increased the efficiency of salt removal to 93% compared with 25% in CNT electrodes alone.

*4.2.3.5. Challenges and opportunities of application of CNT and graphene in desalination*

Novel composite membranes containing NPG/GO and CNT can be divided into two categories: membranes made of only CNTs/NPG/GO known as freestanding membranes and polymeric/ceramic membranes modified with these nanomaterials. Modification of polymeric membranes can be made either by the introduction of nanomaterial on a membrane surface or its addition to a membrane casting solution followed by membrane formation from a mixture of a polymer and a nanomaterial.

Polymeric or ceramic membranes containing NPG/GO and CNT used in pressure-driven processes characterize by high water/permeate flux and possess antifouling and antibacterial properties as well as high mechanical and thermal stability. The flux of nanomembranes is higher than conventional RO or NF membranes, while the retention of low molecular weight compounds is similar. The efficiency of such membranes is beneficial in regard to the removal of dyes, separation of monovalent ions from bivalent ones and dewatering of water-solvent mixtures. Additionally, membranes containing carbon-based nanomaterials have been successfully applied to desalination with FO, MD and CDI, due to their stability and high efficiency.

Various synthesis of VA-CNT and graphene freestanding membranes are complicated and research needs for fabricating them on a large scale. Therefore, given their productivity and cost, synthesizing these membranes may not be practical for industrial use at the current time. The potential use of mixed nanocomposite membranes could offer a more feasible alternative compared to freestanding membranes especially when functionalized with appropriate functional groups to enhance performance and their tolerance to fouling. Studies did show that this modification and combination of polymers and nanocarbon materials did enhance the desalination performance compared to conventional desalination techniques. However, there are still limitations associated with the preparation of controllable composite with CNTs/NPG/GO that have consistent properties.

The future development of membranes containing NPG/GO and CNT should be focused on separation efficiency improvement using different production strategies. A lot of effort should be also dedicated to proper recognition of the role and interaction mechanism between graphene or CNT with a membrane. GO and CNT are promising materials for the preparation of membranes for water desalination, but more attention should be given to their disadvantages like mechanical instability, aggregation, non-uniform distribution and surface damages. Additionally, scaling up related to industrial production of commercial ultrathin membranes of high capacity made of graphene is one of the greatest scientific and technical challenges. If successful, the use of such membranes at an industrial scale will lead to significant energy saving in RO installation as well as in other processes. The key to success is to find the balance between production costs and manufacture simplicity. Additionally, such membranes should be resistant to fouling and scaling, which assures high flux long-term operation and savings in operational and capital costs. Moreover, the release of nanomaterials from the membrane and their eventual toxicity should be carefully investigated, especially in regard to their practical use in desalination processes.

# References

[1] H. March, D. Saur, A.M. Rico-Amorós, The end of scarcity? Water desalination as the new cornucopia for Mediterranean Spain, J. Hydrol., 519 (2014) 2642–2651.

[2] P.S. Goh, A.F. Ismail, N. Hilal, Nano-enabled membranes technology: sustainable and revolutionary solutions for membrane desalination?, Desalination, 380 (2016) 100–104.

[3] R. Baten, K. Stummeyer, How sustainable can desalination be?, Desal. Water Treat., 51 (2013) 44–52.

[4] S. Miller, H. Shemer, R. Semiat, Energy and environmental issues in desalination, Desalination, 366 (2015) 2–8.

[5] B.M. Haddad, A case for an ecological–economic research program for desalination, Desalination, 324 (2013) 72–78.

[6] N. Voutchkov, Energy use for membrane seawater desalination – current status and trends, Desalination, 431 (2018) 2–14.

[7] N. Voutchkov, R. Bergman, Chapter 3 – Facility Design and Construction, in: Reverse Osmosis and Nanofiltration, Manual of Water Supply Practices M 46, 2nd ed., AWWA, Denver, USA, 2007, pp. 63–163.

[8] M.H.I. Dore, Forecasting the economic costs of desalination technology, Desalination, 172 (2005) 207–214.

[9] K.P. Lee, T.C. Arnot, D. Mattia, A review of reverse osmosis membrane materials for desalination—development to date and future potential, J. Membr. Sci., 370 (2011) 1–22.

[10] G. Amy, N. Ghaffour, Z.Y. Li, L. Francis, R.V. Linares, T. Missimer, S. Lattemann, Membrane-based seawater desalination: present and future prospects, Desalination, 401 (2017) 16–21.

[11] S. Raghavendra, Hebbar, A.M. Isloor, Inamuddin, A.M. Asiri, Carbon nanotube- and graphene-based advanced membrane materials for desalination, Environ. Chem. Lett., 15 (2017) 643–671.

[12] S.S. Shenvi, A.M. Isloor, A.F. Ismail, A review on RO membrane technology: developments and challenges, Desalination, 368 (2015) 10–26.

[13] B.J. Hinds, N. Chopra, T. Rantell, R. Andrews, V. Gavalas, L.G. Bachas, Aligned multiwalled carbon nanotube membranes, Science, 303 (2004) 62–65.

[14] M. Bodzek, K. Konieczny, A. Kwiecińska-Mydlak, The application for nanotechnology and nanomaterials in water and wastewater treatment: membranes, photocatalysis and disinfection, Desal. Water Treat., 186 (2020) 88–106.

[15] M. Bodzek, K. Konieczny, A. Kwiecińska-Mydlak, Nanotechnology in water and wastewater treatment. Graphene – the nanomaterial for next generation of semipermeable membranes, Crit. Rev. Env. Sci., 50 (2020) 1515–1579.

[16] M. Majumder, P. Ajayan, Carbon Nanotube Membranes: A New Frontier in Membrane Science, E. Drioli, L. Giorno, Eds., Comprehensive Membrane Science and Engineering, Vol. 1, Elsevier, 2010, pp. 291–310.

[17] S.T. Hsu, K.T. Cheng, J.S. Chiou, Seawater desalination by direct contact membrane distillation, Desalination, 143 (2002) 279–287.

[18] M. Sadrzadeh, T. Mohammadi, Seawater desalination using electrodialysis, Desalination, 221 (2008) 440–447.

[19] Y. Oren, Capacitive deionization (CDI) for desalination and water treatment past, present and future (a review), Desalination, 228 (2008) 10–29.

[20] R. Valladares Linares, Z. Li, S. Sarp, S.S. Bucs, G. Amy, J.S. Vrouwenvelder, Forward osmosis niches in seawater desalination and wastewater reuse, Water Res., 66 (2014) 122–139.

[21] J. MacHarg, T.F. Seacord, B. Sessions, ADC baseline tests reveal trends in membrane performance, Int. Desal. Water Reuse Quart., 18 (2008) 30–39.

[22] N. Ghaffour, T.M. Missimer, G.L. Amy, Technical review and evaluation of the economics of water desalination: current and future challenges for better water supply sustainability, Desalination, 309 (2013) 197–207.

[23] N. Voutchkov, Considerations for selection of seawater filtration pretreatment system, Desalination, 261 (2010) 354–364.

[24] L.O. Villacorte, A.A. Tabatabai, D.M. Anderson, G.L. Amy, J.C. Schippers, M.D. Kennedy, Seawater reverse osmosis desalination and (harmful) algal blooms, Desalination, 360 (2015) 61–80.

[25] T.M. Missimer, N. Ghaffour, A.H.A. Dehwah, R.G. Maliva, G. Amy, Subsurface intakes for seawater reverse osmosis facilities: capacity limitation, water quality improvement, and economics, Desalination, 322 (2013) 37–51.

[26] K. Rahmawati, N. Ghaffour, C. Aubry, G.L. Amy, Boron removal efficiency from Red Sea water using different SWRO/BWRO membranes, J. Membr. Sci., 423–424 (2012) 522–529.

[27] S. Lattemann, M.D. Kennedy, G. Amy, Seawater desalination — a green technology?, J. Water Supply Res. Technol. AQUA, 59 (2010) 134–151.

[28] N. Ghaffour, S. Lattemann, T. Missimer, S. Sinha, G. Amy, Renewable energy-driven innovative energy-efficient desalination technologies, Appl. Energy, 136 (2014) 1155–1165.

[29] R.J. Petersen, J.E. Cadotte, Thin-film Composite Reverse Osmosis Membrane, M.C. Porter, Ed., Handbook of Industrial Membrane Technology, Noyes Publication, New Jersey, 1990.

[30] J.E. Cadotte, Reverse Osmosis Membrane, Patent Application No. 4039440, 1977.

[31] A. Fane, C. Tang, R. Wang, Membrane technology for water: microfiltration, ultrafiltration, nanofiltration, and reverse osmosis, Treatise Water Sci., 4 (2011) 301–335.

[32] J.R. Werber, C.O. Osuji, M. Elimelech, Materials for next-generation desalination and water purification membranes, Nat. Rev. Mater., 1 (2016) 16018.

[33] B.J.A. Tarboush, D. Rana, T. Matsuura, H.A. Arafat, R.M. Narbaitz, Preparation of thin-film-composite polyamide membranes for desalination using novel hydrophilic surface modifying macromolecules, J. Membr. Sci., 325 (2008) 166–175.

[34] M.M. Pendergast, E.M.V. Hoek, A review of water treatment membrane nanotechnologies, Energy Environ. Sci., 4 (2011) 1946.

[35] Y. Wang, R. Ou, Q. Ge, H. Wang, T. Xu, Preparation of polyethersulfone/carbon nanotube substrate for high-performance forward osmosis membrane, Desalination, 330 (2013) 70–78.

[36] S. Zhao, L. Zou, Relating solution physicochemical properties to internal concentration polarization in forward osmosis, J. Membr. Sci., 379 (2011) 459–467.

[37] T.S. Chung, L. Luo, C.F. Wan, Y. Cui, G. Amy, What is next for forward osmosis (FO) and pressure retarded osmosis (PRO), Sep. Purif. Technol., 156 (2015) 856–860.

[38] P. Sukitpaneenit, T.S. Chung, High performance thin-film composite forward osmosis hollow fiber membranes with macrovoid-free and highly porous structure for sustainable water production, Environ. Sci. Technol., 46 (2012) 7358–7365.

[39] R.L. McGinnis, N.T. Hancock, M.S. Nowosielski-Slepowron, G.D. McGurgan, Pilot demonstration of the $NH_3/CO_2$ forward osmosis desalination process on high salinity brines, Desalination, 312 (2013) 67–74.

[40] M. Elimelech, W. Philip, The future of seawater desalination: energy, technology, and the environment, Science, 333 (2011) 712.

[41] R. McGovern, J. Lienhard, On the potential of forward osmosis to energetically outperform reverse osmosis desalination, J. Membr. Sci., 469 (2014) 245–250.

[42] N.T. Hancock, N.D. Black, T.Y. Cath, A comparative life cycle assessment of hybrid osmotic dilution desalination and established seawater desalination and wastewater reclamation processes, Water Res., 46 (2012) 1145–1154.

[43] R. Valladares Linares, Z. Li, M. Abu-Ghdaib, C.H. Wei, G.L. Amy, J.S. Vrouwenvelder, Water harvesting from municipal wastewater via osmotic gradient: an evaluation of process performance, J. Membr. Sci., 447 (2013) 50–56.

[44] R. Valladares Linares, Z. Li, V. Yangali-Quintanilla, N. Ghaffour, G. Amy, T. Leiknes, H. Vrouwenvelder, Life cycle cost of a hybrid forward osmosis – low pressure reverse osmosis (FO–LPRO) system for seawater desalination and wastewater recovery, Water Res., 88 (2016) 225–234.

[45] D.L. Shaefer, J.R. Werber, H. Jaramillo, S. Lin, M. Elimelech, Forward osmosis: where are we now?, Desalination, 356 (2015) 271–284.

[46] S. Adham, A. Hussain, J.M. Matar, R. Dores, A. Janson, Application of membrane distillation for desalting brines from thermal desalination plants, Desalination, 314 (2013) 101–108.

[47] A. Alkhudhiri, N. Darwish, N. Hilal, Membrane distillation: a comprehensive review, Desalination, 287 (2012) 2–18.

[48] L.F. Dumée, K. Sears, J. Schütz, N. Finn, C. Huynh, S. Hawkins, M. Duke, S. Gray, Characterization and evaluation of carbon nanotube Bucky-Paper membranes for direct contact membrane distillation, J. Membr. Sci., 351 (2010) 36–43.

[49] L.M. Camacho, L. Dumée, J. Zhang, J. Li, M. Duke, J. Gomez, S. Gray, Advances in membrane distillation for water desalination and purification applications, Water, 5 (2013) 94–196.

[50] P. Wang, T.S. Chung, A new-generation asymmetric multi-bore hollow fiber membrane for sustainable water production via vacuum membrane distillation, Environ. Sci. Technol., 47 (2013) 6272–6278.

[51] L. Francis, N. Ghaffour, A.S. Alsaadi, S.P. Nunes, G.L. Amy, Performance evaluation of the DCMD process under bench scale and large scale module operating conditions, J. Membr. Sci., 445 (2014) 103–112.

[52] D. Winter, J. Koschikowski, M. Wieghaus, Desalination using membrane distillation: experimental studies on full scale spiral wound modules, J. Membr. Sci., 375 (2011) 104–112.

[53] M.A. Anderson, A.L. Cudero, J. Palma, Capacitive deionization as an electrochemical means of saving energy and delivering clean water. Comparison to present desalination practices: will it compete?, Electrochim. Acta, 55 (2010) 3845–3856.

[54] L. Pan, X. Wang, Y. Gao, Y. Zhang, Y. Chen, Z. Sun, Electrosorption of anions with carbon nanotube and nanofibre composite film electrodes, Desalination, 244 (2009) 139–143.

[55] P. Xu, J.E. Drewes, D. Heil, G. Wang, Treatment of brackish produced water using carbon aerogel-based capacitive deionization technology, Water Res., 42 (2008) 2605–2617.

[56] C.H. Hou, J.F. Huang, H.R. Lin, B.Y. Wang, Preparation of activated carbon sheet electrode assisted electrosorption process, J. Taiwan Inst. Chem. Eng., 43 (2012) 473–479.

[57] C.H. Hou, N.L. Liu, H.L. Hsu, W. Den, Development of multi-walled carbon nanotube/poly(vinyl alcohol) composite as electrode for capacitive deionization, Sep. Purif. Technol., 130 (2014) 7–14.

[58] C. Yan, L. Zou, R. Short, Single-walled carbon nanotubes and polyaniline composites for capacitive deionization, Desalination, 290 (2012) 125–129.

[59] D. Qadir, H. Mukhtar, L.K. Keong, Mixed matrix membranes for water purification applications, Sep. Purif. Rev., 46 (2017) 62–80.

[60] D. Emadzadeh, W.J. Lau, T. Matsuura, M. Rahbari-Sisakht, A.F. Ismail, A novel thin-film composite forward osmosis membrane prepared from $PSf–TiO_2$ nanocomposite substrate for water desalination, Chem. Eng. J., 237 (2014) 70–80.

[61] H. Dong, L. Zhao, L. Zhang, H. Chen, C. Gao, Winston, W.S. Ho, High-flux reverse osmosis membranes incorporated with NaY zeolite nanoparticles for brackish water desalination, J. Membr. Sci., 476 (2014) 373–383.

[62] A. Peyki, A. Rahimpour, M. Jahanshahi, Preparation and characterization of thin-film composite reverse osmosis membranes incorporated with hydrophilic $SiO_2$ nanoparticles, Desalination, 368 (2015) 152–158.

[63] N. Niksefat, M. Jahanshahi, A. Rahimpour, The effect of $SiO_2$ nanoparticles on morphology and performance of thin-film composite membranes for forward osmosis application, Desalination, 343 (2014) 140–146.

[64] R. Das, M.E. Ali, S.B. Abd Hamid, S. Ramakrishna, Z.Z. Chowdhury, Carbon nanotube membranes for water purification: a bright future in water desalination, Desalination, 336 (2014) 97–109.

[65] R. Das, S.B. Abd Hamid, M.E. Ali, A.F. Ismail, M.S.M. Annuar, S. Ramakrishna, Multifunctional carbon nanotubes in water treatment: the present, past and future, Desalination, 354 (2014) 160–179.

[66] P.S. Goh, A.F. Ismail, Graphene-based nanomaterial: the state-of-the-art material for cutting edge desalination technology, Desalination, 356 (2015) 115–128.

[67] K.A. Mahmoud, B. Mansoor, A. Mansour, M. Khraisheh, Functional graphene nanosheets: the next generation membranes for water desalination, Desalination, 356 (2015) 208–225.

[68] I. Akin, E. Zor, H. Bingol, M. Ersoz, Green synthesis of reduced graphene oxide/polyaniline composite and its application for salt rejection by polysulfone based composite membranes, J. Phys. Chem. B, 118 (2014) 5707–5716.

[69] A. Rodríguez-Calvo, G.A. Silva-Castro, F. Osorio, J. González-López, C. Calvo, Novel membrane materials for reverse osmosis desalination, Hydrol. Curr. Res., 5 (2014) 167, doi: 10.4172/2157–7587.1000167.

[70] D.A. Fedosov, A.V. Smirnov, E.E. Knyazeva, I.I. Ivanova, Zeolite membranes: synthesis, properties, and application, Pet. Chem., 51 (2012) 657–667.

[71] J. Coronas, J. Santamaria, State-of-the-art in zeolite membrane reactors, Top. Catal., 29 (2004) 29–44.

[72] M.S. Boroglu, M.A. Gurkaynak, Fabrication and characterization of silica modified polyimide–zeolite mixed matrix membranes for gas separation properties, Polym. Bull., 66 (2010) 463–478.

[73] B. Libby, W.H. Smyrl, E.L. Cussler, Polymer-zeolite composite membranes for direct methanol fuel cells, AIChE J., 49 (2003) 991–1001.

[74] T.C. Bowen, R.D. Noble, J.L. Falconer, Fundamentals and applications of pervaporation through zeolite membranes, J. Membr. Sci., 245 (2004) 1–33.

[75] H. Dong, X.Y. Qu, L. Zhang, L.H. Cheng, H.L. Chen, C.J. Gao, Preparation and characterization of surface-modified zeolite-polyamide thin film nanocomposite membranes for desalination, Desal. Water Treat., 34 (2011) 6–12.

[76] B. Zhu, Z. Hong, N. Milne, C.M. Doherty, L. Zou, Y.S. Lin, Desalination of seawater ion complexes by MFI-type zeolite membranes: temperature and long term stability, J. Membr. Sci., 453 (2014) 126–135.

[77] W. Xu, J. Dong, J. Li, J. Li, F. Wu, A novel method for the preparation of zeolite ZSM-5, J. Chem. Soc., Chem. Commun., 10 (1990) 755–756.

[78] L. Li, J. Dong, T. Nenoff, Transport of water and alkali metal ions through MFI zeolite membranes during reverse osmosis, Sep. Purif. Technol., 53 (2007) 42–48.

[79] L. Li, J. Dong, T.M. Nenoff, R. Lee, Desalination by reverse osmosis using MFI zeolite membranes, J. Membr. Sci., 243 (2004) 401–404.

[80] F. Jareman, J. Hedlund, J. Sterte, Effects of aluminum content on the separation properties of MFI membranes, Sep. Purif. Technol., 32 (2003) 159–163.

[81] M.C. Duke, J. O'Brien-Abraham, N. Milne, B. Zhu, J.Y.S. Lin, J.C. Diniz da Costa, Seawater desalination performance of MFI type membranes made by secondary growth, Sep. Purif. Technol., 68 (2009) 343–350.

[82] L. Li, N. Liu, B. McPherson, R. Lee, Enhanced water permeation of reverse osmosis through MFI-type zeolite membranes with high aluminum contents, Ind. Eng. Chem. Res., 46 (2007) 1584–1589.

[83] J. Lu, N. Liu, L. Li, R. Lee, Organic fouling and regeneration of zeolite membrane in wastewater treatment, Sep. Purif. Technol., 72 (2010) 203–207.

[84] M. Kazemimoghadam, New nanopore zeolite membranes for water treatment, Desalination, 251 (2010) 176–180.

[85] M. Fathizadeh, A. Aroujalian, A. Raisi, Effect of added NaX nano-zeolite into polyamide as a top thin layer of membrane on water flux and salt rejection in a reverse osmosis process, J. Membr. Sci., 375 (2011) 88–95.

[86] N. Liu, L. Li, B. McPherson, R. Lee, Removal of organics from produced water by reverse osmosis using MFI-type zeolite membranes, J. Membr. Sci., 325 (2008) 357–361.

[87] S.M. Rassoulinejad-Mousavi, J. Azamat, A. Khataee, Y. Zhang, Molecular dynamics simulation of water purification using zeolite MFI nanosheets, Sep. Purif. Technol., 234 (2020) 116080, https://doi.org/10.1016/j.seppur.2019.116080.

[88] F. Liu, B.-R. Ma, D. Zhou, Y. Xiang, L. Xue, Breaking through tradeoff of polysulfone ultrafiltration membranes by zeolite 4A, Microporous Mesoporous Mater., 186 (2014) 113–120.

[89] R. Han, S. Zhang, C. Liu, Y. Wang, X. Jian, Effect of NaA zeolite particle addition on poly(phthalazinone ether sulfone ketone) composite ultrafiltration (UF) membrane performance, J. Membr. Sci., 345 (2009) 5–12.

[90] D. Kunnakorn, T. Rirksomboon, P. Aungkavattana, N. Kuanchertchoo, D. Atong, S. Kulprathipanja, Performance of sodium A zeolite membranes synthesized via microwave and autoclave techniques for water–ethanol separation: recycle continuous pervaporation process, Desalination, 269 (2011) 78–83.

[91] P. Swenson, B. Tanchuk, E. Bastida, W. An, S.M. Kuznicki, Water desalination and de-oiling with natural zeolite membranes — potential application for purification of SAGD process water, Desalination, 286 (2012) 442–446.

[92] J. Caro, M. Noack, Zeolite membranes — recent developments and progress, Microporous Mesoporous Mater., 115 (2008) 215–233.

[93] J. Caro, M. Noack, P. Kolsch, R. Schafer, Zeolite membranes - state of their development and perspective, Microporous Mesoporous Mater., 38 (2000) 3–24.

[94] H. Huang, X. Qu, X. Ji, X. Gao, L. Zhang, H. Chen, L. Hoi, Acid and multivalent ion resistance of thin film nanocomposite RO membranes loaded with silicalite-1 nanozeolites, J. Mater. Chem. A, 1 (2013) 11343–11349.

[95] M. Pera-Titus, C. Fite, V. Sebastia, E. Lorente, J. Llorens, F. Cunill, Modeling pervaporation of ethanol/water mixtures within "real" zeolite NaA membranes, Ind. Eng. Chem. Res., 47 (2008) 3213–3224.

[96] S. Turgman-Cohen, J.C. Araque, E.M.V. Hoek, F.A. Escobedo, Molecular dynamics of equilibrium and pressure-driven transport properties of water through LTA-type zeolites, Langmuir, 29 (2013) 12389–12399.

[97] Z. Hu, Y. Chen, J. Jiang, Zeolitic imidazolate framework-8 as a reverse osmosis membrane for water desalination: insight from molecular simulation, J. Chem. Phys., 134 (2011) 134705, https://doi.org/10.1063/1.3573902.

[98] M. Tian, Y.N. Wang, R. Wang, Synthesis and characterization of novel high-performance thin film nanocomposite (TFN) FO membranes with nanofibrous substrate reinforced by functionalized carbon nanotubes, Desalination, 370 (2015) 79–86.

[99] S.P. Surwade, S.N. Smirnov, I.V. Vlassiouk, R.R. Unocic, G.M. Veith, S. Dai, S.M. Mahurin, Water desalination using nanoporous single-layer graphene, Nat. Nanotechnol., 10 (2015) 459–464.

[100] D. Cohen-Tanugi, J.C. Grossman, Nanoporous graphene as a reverse osmosis membrane: recent insights from theory and simulation, Desalination, 366 (2015) 59–70.

[101] J. Wang, P. Zhang, B. Liang, Y. Liu, T. Xu, L. Wang, B. Cao, K. Pan, Graphene oxide as an effective barrier on a porous nanofibrous membrane for water treatment, ACS Appl. Mater. Interfaces, 8 (2016) 6211–6218.

[102] M. Hu, B. Mi, Enabling graphene oxide nanosheets as water separation membranes, Environ. Sci. Technol., 47 (2013) 3715–3723.

[103] J.K. Holt, H.G. Park, Y. Wang, M. Stadermann, A.B. Artyukhin, C.P. Grigoropoulos, A. Noy, O. Bakajin, Fast mass transport through sub-2-nanometer carbon nanotubes, Science, 312 (2006) 1034–1037.

[104] J. Abraham, K.S. Vasu, C.D. Williams, K. Gopinadhan, Y. Su, C.T. Cherian, J. Dix, E. Prestat, S.J. Haigh, I.V. Grigorieva, P. Carbone, A.K. Geim, R.R. Nair, Tunable sieving of ions using graphene oxide membranes, Nat. Nanotechnol., 12 (2017) 546–550.

[105] K. Sears, L. Dumée, J. Schütz, M. She, C. Huynh, S. Hawkins, M. Duke, S. Gray, Recent developments in carbon nanotube membranes for water purification and gas separation, Materials, 3 (2010) 127–149.

[106] M. Rashid, S.F. Ralph, Carbon nanotube membranes: synthesis, properties, and future filtration applications, Nanomaterials, 7 (2017) 1–28.

[107] J.A. Thomas, A.J.H. McGaughey, Water flow in carbon nanotubes: transition to subcontinuum transport, Phys. Rev. Lett., 102 (2009) 184502.

[108] R.H. Tunuguntla, R.Y. Henley, Y.C. Yao, T.A. Pham, M. Wanunu, A. Noy, Enhanced water permeability and tunable ion selectivity in subnanometer carbon nanotube porins, Science, 357 (2017) 792–796.

[109] B. Corry, Water and ion transport through functionalised carbon nanotubes: implications for desalination technology, Energy Environ Sci., 4 (2011) 751–759.

[110] Y. Chan, J.M. Hill, Ion selectivity using membranes comprising functionalized carbon nanotubes, J. Math. Chem., 53 (2013) 1258–1273.

[111] C.H. Ahn, Y. Baek, C. Lee, S.O. Kim, S. Kim, S. Lee, Carbon nanotube-based membranes: fabrication and application to desalination, J. Ind. Eng. Chem., 18 (2012) 1551–1559.

[112] G. Hummer, J.C. Rasaiah, J.P. Noworyta, Water conduction through the hydrophobic channel of a carbon nanotube, Nature, 414 (2001) 188–190.

[113] A.S. Brady-Estévez, S. Kang, M. Elimelech, A single-walled-carbon-nanotube filter for removal of viral and bacterial pathogens, Small, 4 (2008) 481–484.

[114] X. Peng, J. Jin, E.M. Ericsson, I. Ichinose, General method for ultrathin free-standing films of nanofibrous composite materials, J. Am. Chem. Soc., 129 (2007) 8625–8633.

[115] L. Zhang, G.Z. Shi, S. Qiu, L.H. Cheng, H.L. Chen, Preparation of high-flux thin film nanocomposite reverse osmosis membranes by incorporating functionalized multi-walled carbon nanotubes, Desal. Water Treat., 34 (2011) 19–24.

[116] S. Kar, R.C. Bindal, P.K. Tewari, Carbon nanotube membranes for desalination and water purification: challenges and opportunities, Nano Today, 7 (2012) 385–389.

[117] S.M. Park, J. Jung, S. Lee, Y. Baek, J. Yoon, D.K. Seo, Fouling and rejection behavior of carbon nanotube membranes, Desalination, 343 (2014) 180–186.

[118] M. Bhadra, S. Roy, S. Mitra, Enhanced desalination using carboxylated carbon nanotube immobilized membranes, Sep. Purif. Technol., 120 (2013) 373–377.

[119] F. Fornasiero, H.G. Park, J.K. Holt, M. Stadermann, C.P. Grigoropoulos, A. Noy, Ion exclusion by sub-2-nm carbon nanotube pores, Proc. Natl. Acad. Sci., 105 (2008) 17250–17255.

[120] C.F. de Lannoy, E. Soyer, M.R. Wiesner, Optimizing carbon nanotube-reinforced polysulfone ultrafiltration membranes through carboxylic acid functionalization, J. Membr. Sci., 447 (2013) 395–402.

[121] W.F. Chan, H.Y. Chen, A. Surapathi, M.G. Taylor, X. Shao, E. Marand, J.K. Johnson, Zwitterion functionalized carbon nanotube/polyamide nanocomposite membranes for water desalination, ACS Nano, 7 (2013) 5308–5319.

[122] M.A. Tofighy, T. Mohammadi, Adsorption of divalent heavy metal ions from water using carbon nanotube sheets, J. Hazard. Mater., 185 (2011) 140–147.

[123] M.S. Mauter, M. Elimelech, Environmental applications of carbon-based nanomaterials, Environ. Sci. Technol., 42 (2008) 5843–5859.

[124] L. Dumee, J.L. Campbell, K. Sears, J. Schutz, N. Finn, M. Duke, S. Gray, The Impact of hydrophobic coating on the performance of carbon nanotube bucky paper membranes in membrane distillation, Desalination, 283 (2011) 64–67.

[125] Y. You, V. Sahajwalla, M. Yoshimura, R.K. Joshi, Graphene and graphene oxide for desalination, Nano, 8 (2016) 117–119.

[126] R. Nair, H. Wu, P. Jayaram, I. Grigorieva, A. Geim, Unimpeded permeation of water through helium-leak–tight graphene-based membranes, Science, 335 (2012) 442–444.

[127] N. Songa, X. Gao, Z. Mac, X. Wanga, Y. Weia, C. Gao, A review of graphene-based separation membrane: materials, characteristics, preparation and applications, Desalination, 437 (2018) 59–72.

[128] S. Stankovich, D.A. Dikin, R.D. Piner, K.A. Kohlhaas, A. Kleinhammes, Y. Jia, Y. Wu, S.T. Nguyen, R.S. Ruoff, Synthesis of graphene-based nanosheets via chemical reduction of exfoliated graphite oxide, Carbon, 45 (2007) 1558–1565.

[129] M. Hu, B. Mi, Layer-by-layer assembly of graphene oxide membranes via electrostatic interaction, J. Membr. Sci., 469 (2014) 80–87.

[130] X. Wang, Z. Xiong, Z. Liu, T. Zhang, Exfoliation at the liquid/air Interface to assembler reduced graphene oxide ultrathin films for a flexible noncontact sensing device, Adv. Mater., 27 (2015) 1370–1375.

[131] X. Chen, G. Liu, H. Zhang, Y. Fan, Fabrication of graphene oxide composite membranes and their application for pervaporation dehydration of butanol, Chin. J. Chem. Eng., 23 (2015) 1102–1109.

[132] M.J. McAllister, J.L. Li, D.H. Adamson, H.C. Schniepp, A.A. Abdala, J. Liu, M. Herrera-Alonso, D.L. Milius, R. Car, R.K. Prud'homme, I.K. Aksay, Single sheet functionalized graphene by oxidation and thermal expansion of graphite, Chem. Mater., 19 (2007) 4396–4404.

[133] J. Borges, J.F. Mano, Molecular interactions driving the layer-by-layer assembly of multilayers, Chem. Rev., 114 (2014) 8883–8942.

[134] Y. Xiang, S. Lua, S.P. Jiang, Layer-by-layer self-assembly in the development of electrochemical energy conversion and storage devices from fuel cells to supercapacitors, Chem. Soc. Rev., 41 (2012) 7291–7321.

[135] W.L. Xu, C. Fang, F. Zhou, Z. Song, Q. Liu, R. Qiao, M. Yu, Self-assembly: a facile way of forming ultrathin, high-performance graphene oxide membranes for water purification, Nano Lett., 17 (2017) 2928–2933.

[136] C. Yu, B. Zhang, F. Yana, J. Zhao, J. Li, L. Li, J. Li, Engineering nanoporous graphene oxide by hydroxyl radicals, Carbon, 105 (2016) 291–296.

[137] B. Mi, Graphene oxide membranes for ionic and molecular sieving, Science, 343 (2014) 740–742.

[138] Y. Yuan, X. Gao, Y. Wei, X. Wang, J. Wang, Y. Zhang, C. Gao, Enhanced desalination performance of carboxyl functionalized graphene oxide nanofiltration membranes, Desalination, 405 (2017) 29–39.

[139] A. Nicolaï, B.G. Sumpter, V. Meunier, Tunable water desalination across graphene oxide framework membranes, Phys. Chem. Chem. Phys., 16 (2014) 8646–8654.

[140] D. Cohen-Tanugi, J.C. Grossman, Water desalination across nanoporous graphene, Nano Lett., 12 (2012) 3602–3608.

[141] Y. Han, Z. Xu, C. Gao, Ultrathin graphene nanofiltration membrane for water purification, Adv. Funct. Mater., 23 (2013) 3693–3700.

[142] R.K. Joshi, P. Carbone, F.C. Wang, V.G. Kravets, Y. Su, I.V. Grigorieva, H.A. Wu, A.K. Geim, R.R. Nair, Precise and ultrafast molecular sieving through graphene oxide membranes, Science, 343 (2014) 752–754.

[143] C. Xu, A. Cui, Y. Xu, X. Fu, Graphene oxide–TiO$_2$ composite filtration membranes and their potential application for water purification, Carbon, 62 (2013) 465–471.

[144] N. Wang, S. Ji, G. Zhang, J. Li, L. Wang, Self-assembly of graphene oxide and polyelectrolyte complex nanohybrid membranes for nanofiltration and pervaporation, Chem. Eng. J., 213 (2012) 318–329.

[145] P. Sun, M. Zhu, K. Wang, M. Zhong, J. Wei, D. Wu, Z. Xu, H. Zhu, Selective ion penetration of graphene oxide membranes, ACS Nano, 7 (2012) 428–437.

[146] S. Xia, M. Ni, Preparation of polyvinylidene fluoride membranes with graphene oxide addition for natural organic matter removal, J. Membr. Sci., 473 (2015) 54–62.

[147] M.E.A. Ali, L. Wang, X. Wang, X. Feng, Thin-film composite membranes embedded with graphene oxide for water desalination, Desalination, 386 (2016) 67–76.

[148] H.M. Hegab, L. Zou, Graphene oxide-assisted membranes: fabrication and potential applications in desalination and water purification, J. Membr. Sci., 484 (2015) 95–106.

[149] Y. Manawi, V. Kochkodan, M. Ali Hussein, M.A. Khaleel, M. Khraisheh, N. Hilal, Can carbon-based nanomaterials revolutionize membrane fabrication for water treatment and desalination?, Desalination, 391 (2016) 69–88.

[150] Z. Yang, X.H. Ma, C.Y. Tang, Recent development of novel membranes for desalination, Desalination, 434 (2018) 37–59.

[151] A. Anand, B. Unnikrishnan, J.Y. Mao, H.J. Lin, C.C. Huang, Graphene-based nanofiltration membranes for improving salt rejection, water flux and antifouling – a review, Desalination, 429 (2018) 119–133.

[152] F. Perreault, M.E. Tousley, M. Elimelech, Thin-film composite polyamide membranes functionalized with biocidal graphene oxide nanosheets, Environ. Sci. Technol. Lett., 1 (2014) 71–76.

[153] W. Choi, J. Choi, J. Bang, J.H. Lee, Layer-by-layer assembly of graphene oxide nanosheets on polyamide membranes for durable reverse-osmosis applications, ACS Appl. Mater. Interfaces, 5 (2013) 12510–12519.

[154] S. Liu, T.H. Zeng, M. Hofmann, E. Burcombe, J. Wei, R. Jiang, Antibacterial activity of graphite, graphite oxide, graphene oxide, and reduced graphene oxide: membrane and oxidative stress, ACS Nano, 5 (2011) 6971–6980.

[155] S. Wang, S. Liang, P. Liang, X. Zhang, J. Sun, S. Wu, X. Huang, In-situ combined dual-layer CNT/PVDF membrane for electrically-enhanced fouling resistance, J. Membr. Sci., 491 (2015) 37–44.

[156] Y. Wang, J. Zhu, H. Huang, H.H. Cho, Carbon nanotube composite membranes for microfiltration of pharmaceuticals and personal care products: capabilities and potential mechanisms, J. Membr. Sci., 479 (2015) 165–174.

[157] V. Vatanpour, N. Zoqi, Surface modification of commercial seawater reverse osmosis membranes by grafting of hydrophilic monomer blended with carboxylated multiwalled carbon nanotubes, Appl. Surf. Sci., 396 (2017) 1478–1489.

[158] M. Adamczak, G. Kamińska, J. Bohdziewicz, Preparation of polymer membranes by *in-situ* interfacial polymerization, Int. J. Polym. Sci., 2019 (2019) 6217924, 13 pages, https://doi.org/10.1155/2019/6217924.

[159] J. Yin, G. Zhu, B. Deng, Graphene oxide (GO) enhanced polyamide (PA) thin-film nanocomposite (TFN) membrane for water purification, Desalination, 379(2016) 93–101.

[160] K. Xu, B. Feng, C. Zhou, A. Huang, Synthesis of highly stable graphene oxide membranes on polydopamine functionalized supports for seawater desalination, Chem. Eng. Sci., 146 (2016) 159–165.

[161] S.G. Kim, D.H. Hyeon, J.H. Chun, B.H. Chun, S.H. Kim, Novel thin nanocomposite RO membranes for chlorine resistance, Desal. Water Treat., 51 (2013) 6338–6345.

[162] V. Kochkodan, D.J. Johnson, N. Hilal, Polymeric membranes: surface modification for minimizing (bio)colloidal fouling, Adv. Colloid Interface Sci., 206 (2014) 116–140.

[163] Y. Tu, M. Lv, P. Xiu, T. Huynh, M. Zhang, M. Castelli, Destructive extraction of phospholipids from *Escherichia coli* membranes by graphene nanosheets, Nat. Nanotechnol., 8 (2013) 594–601.

[164] X.F. Sun, J. Qin, P.F. Xia, B.B. Guo, C.M. Yang, C. Song, S.G. Wang, Graphene oxide–silver nanoparticle membrane for biofouling control and water purification, Chem. Eng. J., 281 (2015) 53–59.

[165] W. Ma, A. Soroush, T. Van Anh Luong, S. Rahaman, Cysteamine- and graphene oxide-mediated copper nanoparticle decoration on reverse osmosis membrane for enhanced anti-microbial performance, J. Colloid Interface Sci., 501 (2017) 330–340.

[166] G.S. Lai, W.J. Lau, P.S. Goh, A.F. Ismail, N. Yusof, Y.H. Tan, Graphene oxide incorporated thin film nanocomposite nanofiltration membrane for enhanced salt removal performance, Desalination, 387 (2016) 14–24.

[167] S. Bano, A. Mahmood, S.J. Kim, K.H. Lee, Graphene oxide modified polyamide nanofiltration membrane with improved flux and antifouling properties, J. Mater. Chem. A, 3 (2015) 2065–2071.

[168] M. Safarpour, V. Vatanpour, A. Khataee, M. Esmaeili, Development of a novel high flux and fouling-resistant thin-film composite nanofiltration membrane by embedding reduced graphene oxide/TiO₂, Sep. Purif. Technol., 154 (2015) 96–107.

[169] M. Safarpour, A. Khataee, V. Vatanpour, Thin film nanocomposite reverse osmosis membrane modified by reduced graphene oxide/TiO₂ with improved desalination performance, J. Membr. Sci., 489 (2015) 43–54.

[170] J. Wang, X. Gao, J. Wang, Y. Wei, Z. Li, C. Gao, O-(Carboxymethyl)-chitosan nanofiltration membrane surface functionalized with graphene oxide nanosheets for enhanced desalting properties, ACS Appl. Mater. Interfaces, 7 (2015) 4381–4389.

[171] X. Chen, M. Qiu, H. Ding, K. Fu, Y. Fan, A reduced graphene oxide nanofiltration membrane intercalated by well-dispersed carbon nanotubes for drinking water purification, Nano, 8 (2016) 5696–5705.

[172] S.M. Xue, Z.L. Xu, Y.J. Tang, C.H. Ji, Polypiperazine-amide nanofiltration membrane modified by different functionalized multiwalled carbon nanotubes (MWCNTs), ACS Appl. Mater. Interfaces, 8 (2016) 19135–19144.

[173] O.K. Park, N.H. Kim, K.T. Lau, J.H. Lee, Effect of surface treatment with potassium persulfate on dispersion stability of multi-walled carbon nanotubes, Mater. Lett., 64 (2010) 718–721.

[174] K. Balasubramanian, M. Burghard, Chemically functionalized carbon nanotubes, Small, 1 (2005) 180–192.

[175] J. Yin, B. Deng, Polymer-matrix nanocomposite membranes for water treatment, J. Membr. Sci., 479 (2015) 256–275.

[176] T.V. Ratto, J.K. Holt, A.W. Szmodis, Membranes with Embedded Nanotubes for Selective Permeability, Patent Application No. 20100025330, 2010.

[177] H. Zhao, S. Qiu, L. Wu, L. Zhang, H. Chen, C. Gao, Improving the performance of polyamide reverse osmosis membrane by incorporation of modified multi-walled carbon nanotubes, J. Membr. Sci., 450 (2014) 249–256.

[178] H.J. Kim, K. Choi, Y. Baek, D. Kim, J. Shim, J. Yoon, J. Lee, High-Performance reverse osmosis CNT/polyamide nanocomposite membrane by controlled interfacial interactions, ACS Appl. Mater. Interfaces, 6 (2014) 2819–2829.

[179] A. Tiraferri, C.D. Vecitis, M. Elimelech, Covalent binding of single-walled carbon nanotubes to polyamide membranes for antimicrobial surface properties, ACS Appl. Mater. Interfaces, 3 (2011) 2869–2877.

[180] J. Zhang, Z. Xu, M. Shan, B. Zhou, Y. Li, B. Li, J. Niu, X. Qian, Synergetic effects of oxidized carbon nanotubes and graphene oxide on fouling control and anti-fouling mechanism of polyvinylidene fluoride ultrafiltration membranes, J. Membr. Sci., 448 (2013) 81–92.

[181] L. Madhura, S. Kanchi, M.I. Sabela, S. Singh, K. Bisetty, Inamuddin, Membrane technology for water purification, Environ. Chem. Lett., 16 (2018) 343–365.

[182] M. Bodzek, Membrane separation techniques – removal of inorganic and organic admixtures and impurities from water environment – review, Arch. Environ. Prot., 45 (2019) 4–19.

[183] B.M. Ganesh, A.M. Isloor, A.F. Ismail, Enhanced hydrophilicity and salt rejection study of graphene oxide-polysulfone mixed matrix membrane, Desalination, 313 (2013) 199–207.

[184] J. Lee, H.R. Chae, Y.J. Won, K. Lee, C.H. Lee, H.H. Lee, I.C. Kim, J.M. Lee, Graphene oxide nanoplatelets composite membrane with hydrophilic and antifouling properties for wastewater treatment, J. Membr. Sci., 448 (2013) 223–230.

[185] Z. Xu, J. Zhang, M. Shan, Y. Li, B. Li, J. Niu, B. Zhou, X. Qian, Organosilane functionalized graphene oxide for enhanced antifouling and mechanical properties of polyvinylidene fluoride ultrafiltration membranes, J. Membr. Sci., 458 (2014) 1–13.

[186] D. Arockiasamy, S. Lawrence, J. Alam, M. Alhoshan, Carbon nanotubes-blended poly (phenylene sulfone) membranes for ultrafiltration applications, Appl. Water Sci., 3 (2012) 93–103.

[187] J. Choi, J. Jegal, W. Kim, Fabrication and characterization of multi-walled carbon nanotubes/polymer blend membranes, J. Membr. Sci., 284 (2006) 406–415.

[188] P. Shah, C.N. Murthy, Studies on the porosity control of MWCNT/polysulfone composite membrane and its effect on metal removal, J. Membr. Sci., 437 (2013) 90–98.

[189] J. Yin, G. Zhu, B. Deng, Multi-walled carbon nanotubes (MWNTs)/polysulfone (PSU) mixed matrix hollow fiber membranes for enhanced water treatment, J. Membr. Sci., 437 (2013) 237–248.

[190] A. Khalid, A.A. Al-Juhani, O.C. Al-Hamouz, T. Laoui, Z. Khan, M.A. Atieh, Preparation and properties of nanocomposite polysulfone/multi-walled carbon nanotubes membranes for desalination, Desalination, 367 (2015) 134–144.

[191] F. Liu, M.R.M. Abed, K. Li, Preparation and characterization of polyvinylidene fluoride (PVDF) based ultrafiltration membranes using nano γ-Al₂O₃, J. Membr. Sci., 366 (2011) 97–103.

[192] A.M. Dimiev, L.B. Alemany, J.M. Tour, Graphene oxide. Origin of acidity, its instability in water, and a new dynamic structural model, ACS Nano, 7 (2013) 576–588.

[193] N. Pezeshk, D. Rana, R.M. Narbaitz, T. Matsuura, Novel modified PVDF ultrafiltration flat-sheet membranes, J. Membr. Sci., 389 (2012) 280–286.

[194] V. Vatanpour, S.S. Madaeni, R. Moradian, S. Zinadini, B. Astinchap, Novel antibifouling nanofiltration polyethersulfone membrane fabricated from embedding TiO₂ coated multi-walled carbon nanotubes, Sep. Purif. Technol., 90 (2012) 69–82.

[195] H. Zhao, L. Wu, Z. Zhou, L. Zhang, H. Chen, Improving the antifouling property of polysulfone ultrafiltration membrane

by incorporation of isocyanate-treated graphene oxide, Phys. Chem. Chem. Phys., 15 (2013) 9084–9092.

[196] J.N. Coleman, M. Cadek, R. Blake, V. Nicolosi, K.P. Ryan, C. Belton, A. Fonseca, J.B. Nagy, Y.K. Gun'ko, W.J. Blau, High performance nanotube-reinforced plastics: understanding the mechanism of strength increase, Adv. Funct. Mater., 14 (2004) 791–798.

[197] F. Dalmas, L. Chazeau, C. Gauthier, K. Masenelli-Varlot, R. Dendievel, J.Y. Cavaillé, L. Forró, Multiwalled carbon nanotube/polymer nanocomposites: processing and properties, J. Polym. Sci., Part B: Polym. Phys., 43 (2005) 1186–1197.

[198] A. Dufresne, M. Paillet, J.L. Putaux, R. Canet, F. Carmona, P. Delhaes, S. Cui, Processing and characterization of carbon nanotube/poly(styrene-co-butyl acrylate) nanocomposites, J. Mater. Sci., 37 (2002) 3915–3923.

[199] N. Mehwish, A. Kausar, M. Siddiq, High-performance polyvinylidene fluoride/poly (styrene – butadiene – styrene)/ functionalized MWCNTs-SCN-Ag nanocomposite membranes, Iran. Polym. J., 24 (2015) 549–559.

[200] H.A. Shawky, S. Chae, S. Lin, M.R. Wiesner, Synthesis and characterization of a carbon nanotube/polymer nanocomposite membrane for water treatment, Desalination, 272 (2011) 46–50.

[201] M. Amini, M. Jahanshahi, A. Rahimpour, Synthesis of novel thin film nanocomposite (TFN) forward osmosis membranes using functionalized multi-walled carbon nanotubes, J. Membr. Sci., 435 (2013) 233–241.

[202] L. Dumée, J. Lee, K. Sears, B. Tardy, M. Duke, S. Gray, Fabrication of thin-film composite poly(amide)-carbon-nanotube supported membranes for enhanced performance in osmotically driven desalination systems, J. Membr. Sci., 427 (2013) 422–430.

[203] K. Goh, L. Setiawan, L. Wei, W. Jiang, R. Wang, Y. Chen, Fabrication of novel functionalized multi-walled carbon nanotube immobilized hollow fiber membranes for enhanced performance in forward osmosis process, J. Membr. Sci., 446 (2013) 244–254.

[204] J.G. Lee, E.J. Lee, S. Jeong, J. Guo, A.K. An, H. Guo, J. Kim, T. Leiknes, N. Ghaffour, Theoretical modeling and experimental validation of transport and separation properties of carbon nanotube electrospun membrane distillation, J. Membr. Sci., 526 (2017) 395–408.

[205] V. Vatanpour, M. Esmaeili, M. Hossein, D. Abadi, Fouling reduction and retention increment of polyethersulfone nanofiltration membranes embedded by amine-functionalized multi-walled carbon nanotubes, J. Membr. Sci., 466 (2014) 70–81.

[206] E.S. Kim, G. Hwang, M. Gamal El-Din, Y. Liu, Development of nanosilver and multi-walled carbon nanotubes thin-film nanocomposite membrane for enhanced water treatment, J. Membr. Sci., 394–395 (2012) 37–48.

[207] J. Zheng, M. Li, K. Yu, J. Hu, X. Zhang, L. Wang, Sulfonated multiwall carbon nanotubes assisted thin-film nanocomposite membrane with enhanced water flux and anti-fouling property, J. Membr. Sci., 524 (2017) 344–353.

[208] J.-N. Shen, Y.C. Chao, R.H. Min, G.C. Jie, B. Van Der Bruggen, Preparation and characterization of thin-film nanocomposite membranes embedded with poly(methyl methacrylate) hydrophobic modified multiwalled carbon nanotubes by interfacial polymerization, J. Membr. Sci., 442 (2013) 18–26.

[209] L. Shen, S. Xiong, Y. Wang, Graphene oxide incorporated thin-film composite membranes for forward osmosis applications, Chem. Eng. Sci., 143 (2016) 194–205.

[210] L. Jin, Z. Wang, S. Zheng, B. Mi, Polyamide-crosslinked graphene oxide membrane for forward osmosis, J. Membr. Sci., 545 (2018) 11–18.

[211] W.S. Hung, Y.H. Chiao, A. Sengupta, Y.W. Lin, S.R. Wickramasinghe, C.C. Hu, H.A. Tsai, K.R. Lee, J.Y. Lai, Tuning the interlayer spacing of forward osmosis membranes based on ultrathin graphene oxide to achieve desired performance, Carbon, 142 (2019) 337–345.

[212] W. Suwaileh, D. Johnson, S. Khodabakhshi, N. Hilal, Development of forward osmosis membranes modified by cross-linked layer-by-layer assembly for brackish water desalination, J. Membr. Sci., 583 (2019) 267–277.

[213] H. Zarrabi, M. Ehsan, V. Vatanpour, A. Shockravi, M. Safarpour, Improvement in desalination performance of thin film nanocomposite nanofiltration membrane using amine-functionalized multiwalled carbon nanotube, Desalination, 394 (2016) 83–90.

[214] S.H. Kim, T.M. Lee, Performance improvement of membrane distillation using carbon nanotubes, Membr. Water Treat., 7 (2016) 367–375.

[215] M. Bhadra, S. Roy, S. Mitra, Desalination across a graphene oxide membrane via direct contact membrane distillation, Desalination, 378 (2016) 37–43.

[216] C. Athanasekou, A. Sapalidis, I. Katris, E. Savopoulou, K. Beltsios, T. Tsoufis, A. Kaltzoglou, P. Falaras, G. Bounos, M. Antoniou, P. Boutikos, G. Em. Romanos, Mixed matrix PVDF/graphene and composite-skin PVDF/graphene oxide membranes applied in membrane distillation, Polym. Eng. Sci., 59 (2019) E262–E278.

[217] Y. Wimalasiri, L. Zou, Carbon nanotube/graphene composite for enhanced capacitive deionization performance, Carbon N.Y., 59 (2013) 464–471.

[218] Y. Wang, L. Zhang, Y. Wu, S. Xu, J. Wang, Polypyrrole/carbon nanotube composites as cathode material for performance enhancing of capacitive deionization technology, Desalination, 354 (2014) 62–67.

[219] H. Li, Y. Gao, L. Pan, Y. Zhang, Y. Chen, Z. Sun, Electrosorptive desalination by carbon nanotubes and nanofibres electrodes and ion-exchange membranes, Water Res., 42 (2008) 4923–4928.

[220] Y. Liu, L. Pan, X. Xu, T. Lu, Z. Sun, D.H.C. Chua, Enhanced desalination efficiency in modified membrane capacitive deionization by introducing ion-exchange polymers in carbon nanotubes electrodes, Electrochim. Acta, 130 (2014) 619–624.